Multi-response optimization of spice-enriched butterfly pea beverages by ANN and chemometric approaches: linking color attributes, functional properties, and *in vitro* bioaccessibility

Senanur Durgut Malçok*

Department of Food Engineering, Faculty of Agriculture, Bursa Uludağ University, Bursa, Türkiye

***Corresponding Author:** Malçok, S.D., Department of Food Engineering, Faculty of Agriculture, Bursa Uludağ University, Bursa, Türkiye. Email: senanurdurgut@uludag.edu.tr

Academic Editor: B.N. Dar, PhD, Department of Food Technology, Islamic University of Science & Technology, Awantipora, Kashmir, India

Received: 9 April 2026; Accepted: 5 July 2026; Published: 28 August 2026
© 2026 Codon Publications

OPEN ACCESS

ORIGINAL ARTICLE

Abstract

Clitoria ternatea L. flowers are a rich natural source of anthocyanins and phenolic compounds. This study comparatively evaluated 10 butterfly pea tea formulations containing mint, rosemary, fenugreek, cardamom, garlic, chili, and their combinations, and investigated the effects of *in vitro* gastrointestinal digestion on their physicochemical and functional properties. Significant formulation-dependent differences were observed in pH, °Brix, color parameters (L*, a*, b*, C*, and h° [hue angle]), total phenolic content (TPC: 756.30–5,299.33 mg GAE/100 g dry matter (dm)), total monomeric anthocyanin content (TMA: 1.39–4.45 mg/kg), and total antioxidant capacity (DPPH: 237.54–1,799.48 µmol Trolox/g dm and FRAP: 161.80–1,114.53 µmol Trolox/g dm). Multivariate analyses successfully differentiated the formulations, with the first two principal components explaining 65.9% of the total variance and revealing strong associations between phenolic recovery, antioxidant responses, and color attributes. A feed-forward artificial neural network (ANN) model demonstrated strong predictive performance, with a high overall correlation between experimental and predicted responses ($R \approx 0.97$). ANN-based optimization identified the mint-enriched formulation (MI) as the best overall formulation (desirability score: 0.4955), whereas CA-PG exhibited the highest TPC after intestinal digestion (12,813.69 mg GAE/100 g dm).

Keywords: artificial neural network (ANN); bioactive components; *Clitoria ternatea* L.; *in vitro* bioaccessibility; principal component analysis (PCA).

Introduction

Clitoria ternatea L., commonly known as butterfly pea or blue pea flower, is a perennial climbing plant belonging to the Fabaceae family that grows in tropical and subtropical regions (Hasanah *et al.*, 2023; Nair *et al.*, 2015). *C. ternatea* flowers are rich in ternatin-type anthocyanins together with numerous phenolic compounds and flavonoids, which contribute to their characteristic blue color, antioxidant activity, and pH-dependent color transitions (Escher *et al.*, 2020; Maia *et al.*, 2025). One of the most remarkable characteristics of the plant is its ability to exhibit pH-sensitive color changes. Ternatin

ISSN 1757-837X online, DOI 10.15586/qas.v18i3.1650

anthocyanins present in the blue flowers can display different color tones depending on pH; while a blue color is observed under neutral conditions, purple or pink hues can appear in acidic environments. This property is not only an aesthetic characteristic but also offers important application possibilities in food technology. In particular, the ability of these pigments to change color across a wide pH range has made them potential biosensors that can be used as natural pH indicators or in intelligent packaging systems (Hasanah *et al.*, 2023).

The distinctive aspect of this study is that butterfly pea blue tea is addressed within the concept of a 'spice-enriched functional beverage'. The addition of garlic (*Allium sativum* L.) is characterized particularly by the presence of organosulfur compounds such as allicin. Allicin is formed through the alliin/alliinase system and is a reactive thiosulfinate capable of undergoing redox reactions with thiol groups, and it has been reported to possess a broad range of biological activities (Borlinghaus *et al.*, 2014). The rationale for using pepper extract (*Capsicum* spp.) as the pungent component is based on its rich secondary metabolite profile, including capsaicinoids responsible for pungency as well as carotenoids, flavonoids, and volatile compounds (Antonio *et al.*, 2018). In this context, the role of the pungent component in the formulation is not limited solely to sensory 'spiciness', but may also contribute to total antioxidant capacity (TAC) measurements through polyphenol content and redox reactivity.

Aromatic herbs and spices used in butterfly pea-based beverage formulations are considered not only for improving sensory characteristics but also for modulating functional properties due to their phenolic compounds and other secondary metabolites. Mint (*Mentha* spp.) and rosemary (*Salvia rosmarinus*), members of the Lamiaceae family, are rich in rosmarinic acid and other phenolic acids and exhibit strong antioxidant properties. These compounds have the potential to form co-pigmentation interactions with anthocyanins and may therefore influence color intensity and pigment stability. Fenugreek (*Trigonella foenum-graecum*) possesses a phytochemical profile rich in flavonoids, saponins, and alkaloids and contains phenolic metabolites associated with antioxidant activity. Cardamom (*Elettaria cardamomum*) is also rich in volatile oil components and is known as an important spice that enhances the aroma profile of beverages. Considering the different phenolic and secondary metabolite profiles of these botanicals, they may generate distinct interactions in anthocyanin-rich beverage matrices such as butterfly pea tea, potentially affecting color stability, phenolic content, and TAC (Antonio *et al.*, 2018; Borlinghaus *et al.*, 2014; Rababah *et al.*, 2004).

In such complex herbal beverage systems, quality parameters are often shaped by the simultaneous effects of multiple variables. When indicators such as pH, soluble solids content, color parameters (L*, a*, b*, C*, and h°), total phenolic content (TPC), TAC, and total monomeric anthocyanin (TMA) content must be evaluated together, traditional single-variable comparisons may be insufficient to fully reveal the relationships within the dataset. For this reason, multivariate data analysis approaches have been proposed as powerful tools for evaluating relationships among quality characteristics of different formulations in food systems (Buvé *et al.*, 2022). Similarly, artificial neural networks (ANN) are increasingly used to model nonlinear multivariate systems and have been reported to provide higher predictive performance than classical Response Surface Methodology (RSM) in certain food processes.

ANN are computational models inspired by the structure of biological neural systems and are capable of learning nonlinear relationships between multiple input and output variables. Unlike traditional statistical approaches, ANN models can effectively capture complex and nonlinear interactions within multivariate datasets without requiring predefined mathematical relationships. Due to their adaptive learning capability, ANN models have been successfully applied in various food engineering and food quality studies, including process optimization, extraction modeling, drying kinetics, fermentation processes, and prediction of physicochemical properties. Previous studies have demonstrated that ANN models can provide high predictive accuracy, low relative error, and strong correlation coefficients when modeling complex food systems. Therefore, integrating ANN-based modeling into experimental food research can significantly strengthen data interpretation and optimization strategies, particularly when multiple quality parameters are simultaneously evaluated (Shi *et al.*, 2024).

In this context, the present study evaluates butterfly pea blue tea within an integrated framework combining functional beverage development, pigment chemistry, and data-driven optimization. Ten formulations (control, chili–garlic control, and mint-, fenugreek-, rosemary-, and cardamom-enriched samples prepared with and without chili–garlic addition) were comparatively investigated in terms of physicochemical properties (pH and °Brix), color parameters (L*, a*, b*, C*, and h°), TPC, TAC (2,2-diphenyl-1-picrylhydrazyl [DPPH] and ferric reducing antioxidant power [FRAP]), and TMA content. We hypothesized that botanicals

rich in phenolic acids and volatile compounds, particularly mint and rosemary, may improve color characteristics, bioactive composition, TAC, and in vitro bioaccessibility through interactions with anthocyanins, whereas redox-active compounds derived from garlic and Capsicum may contribute to matrix-dependent changes in these quality attributes.

Materials and Methods

Material

Chemicals and reagents

Folin–Ciocalteu reagent, sodium carbonate (Na_2CO_3), gallic acid, ethanol (EtOH), methanol (MeOH), TPTZ and ferric chloride were used to determine TPC and TAC (assays were obtained from Merck, Darmstadt, Germany). DPPH was purchased from Sigma-Aldrich (St. Louis, MO, USA). Folin–Ciocalteu reagent is widely used for the colorimetric determination of total phenolic compounds in plant-derived samples and food matrices.

For *in vitro* gastrointestinal digestion experiments, digestive enzymes, including pepsin, pancreatin, and bile salts, were obtained from Sigma-Aldrich. These enzymes are commonly used in standardized *in vitro* digestion protocols to simulate gastric and intestinal digestion processes in food matrices.

All chemicals and reagents used in the analyses were of analytical grade, and all solutions were prepared using distilled water.

Plant materials

The butterfly pea flowers (*Clitoria ternatea* L.) and all spices used in the study, such as mint (*Mentha* spp.), rosemary (*Salvia rosmarinus* L.), fenugreek (*Trigonella foenum-graecum* L.), cardamom (*Elettaria cardamomum* (L.) *Maton*), garlic (*Allium sativum* L.), and chili pepper (*Capsicum* spp.), were purchased from a local herbal market located in Bursa, Türkiye. The plant materials were visually inspected, cleaned to remove foreign particles, and stored in airtight containers at room temperature until preparation of beverage.

Methods

Production methods

Butterfly pea tea infusion was prepared using the hot water extraction method. First, potable water was heated to its boiling point and allowed to cool to approximately 95°C. Subsequently, 10 g of dried butterfly pea flowers were added to 1 L of hot water, resulting in an infusion with a concentration of 1% (w/v). The mixture was allowed to steep for 15 min to ensure efficient extraction of the water-soluble pigments and phenolic compounds from the plant material. It is well known that infusion temperature and time significantly affect the extraction efficiency of anthocyanins and phenolic compounds of butterfly pea flowers. Previous studies have reported that infusion conditions of 80–100°C for 10–15 min provide effective extraction of phenolic compounds and antioxidant components in butterfly pea tea preparations (Prathumtet *et al.*, 2018).

After infusion period, plant material was removed by filtration and a deep blue butterfly pea extract was obtained.

Spice extracts used in the study were prepared separately for each spice. For this purpose, 1 g of each spice sample was extracted in 100 mL of boiling water, corresponding to an extraction concentration of approximately 1% (w/v). The spices were allowed to extract in hot water for 5 min, after which the mixtures were filtered to remove solid particles and obtain clear spice extracts. For preparing spicy formulations, 1 g of garlic and 1 g of dried red chili pepper were added in the spice material and extracted under the above-mentioned conditions. This process enabled the simultaneous extraction of aromatic compounds and pungent components into aqueous medium.

The prepared spice extracts were subsequently blended with the previously obtained butterfly pea infusion to formulate beverage samples. For this purpose, 50 mL of spice extract was added to 200 mL of butterfly pea infusion. Accordingly, a final beverage formulation contained approximately 20% (v/v) spice extract. All beverage samples were mixed thoroughly to ensure homogeneity and stored under appropriate conditions until further analyses (Figure 1).

Beverage samples were coded according to their formulation. Control butterfly pea tea was denoted as C, while formulations containing garlic and chili pepper were indicated by the suffix PG (pepper–gar lic). Abbreviations RO, FE, MI, and CA represent rosemary (*Salvia rosmarinus*), fenugreek (*Trigonella foenum-graecum*), mint (*Mentha spp.*), and cardamom (*Elettaria cardamomum*), respectively (Figure 2).

Analysis methods

°Brix values

°Brix values of spice-enriched butterfly pea beverages were measured at 20 ± 0.5°C using a digital

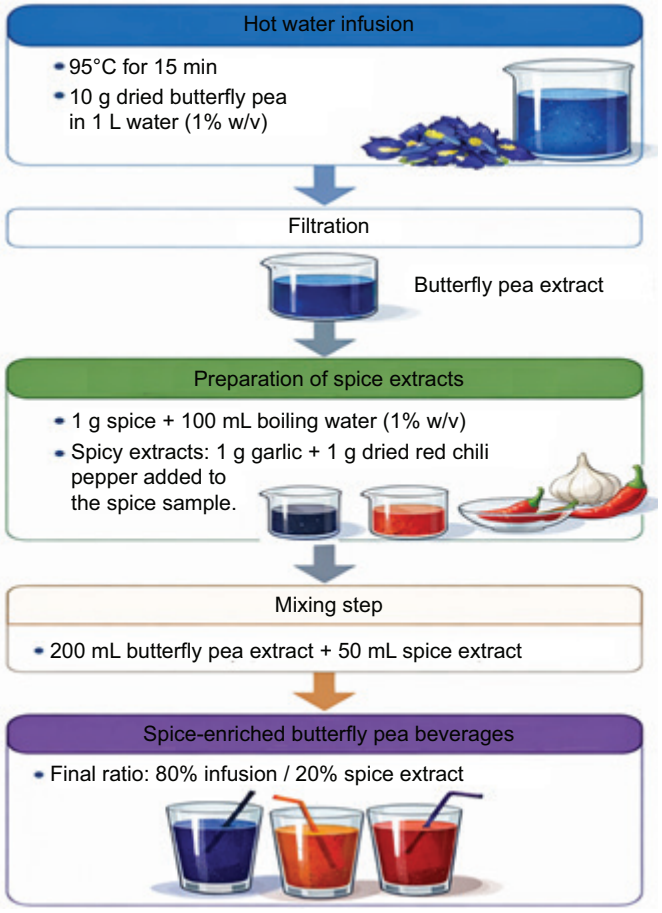

Figure 1. Production method.

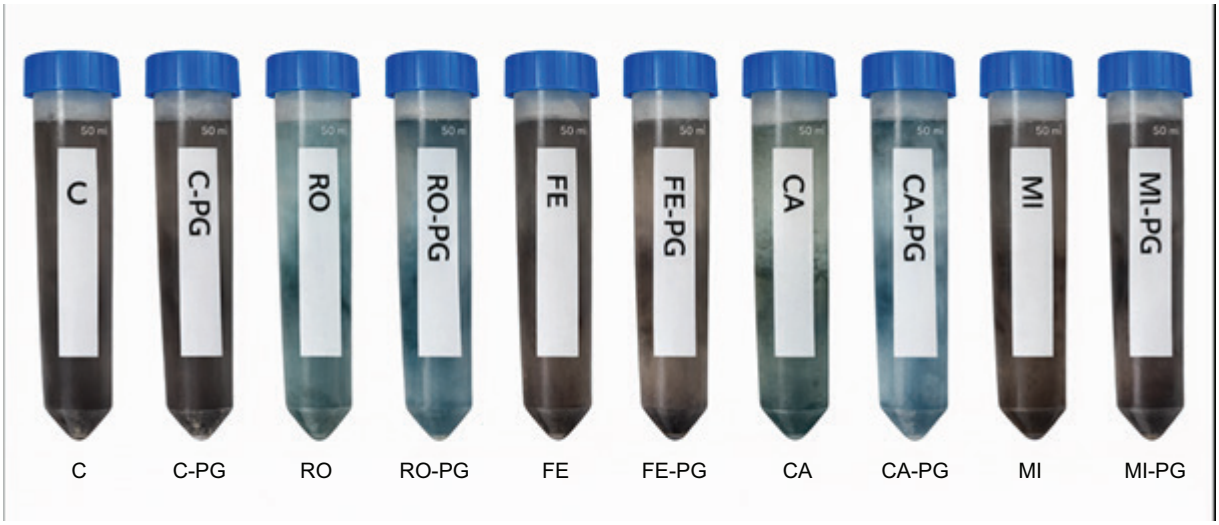

Figure 2. Beverage samples (C = butterfly pea control; C-PG = butterfly pea + pepper + garlic; RO = rosemary extract; RO-PG = rosemary + pepper + garlic; FE = fenugreek extract; FE-PG = fenugreek + pepper + garlic; CA = cardamom extract; CA-PG = cardamom + pepper + garlic; MI = mint extract; MI-PG = mint + pepper + garlic).

refractometer (RFM960 model, Bellingham & Stanley, Tunbridge Wells, UK).

pH values

pH values of butterfly pea beverage samples were determined using a pH meter (SevenCompact model, Mettler Toledo International Inc., Switzerland). Measurements were accomplished under laboratory conditions in order to monitor the acidity characteristics of beverage formulations.

Color

Color parameters of butterfly pea beverages were measured using a Minolta colorimeter (CR-400, Osaka, Japan) according to the method described by Malçok *et al.* (2023). The color values were expressed according to the Commission Internationale de l'Éclairage (CIELAB) color system as L* (lightness), a* (green–red coordinate), and b* (blue–yellow coordinate). In addition, chroma (C*) (Equation 1), representing color intensity, and hue angle (h°) (Equation 2), representing color tone on a 0–360° scale, were calculated in order to obtain a comprehensive evaluation of the color properties of the beverages:

$$C^* = \sqrt{(a^*)^2 + (b^*)^2} \quad (1)$$

$$h^\circ = \tan^{-1}\left(\frac{b^*}{a^*}\right) \quad (2)$$

Extraction for spectrophotometric total antioxidant activity, total phenolic content

Spectrophotometric analyses, such as TPC and TAC were performed using liquid samples of butterfly pea beverages. However, the raw materials used in beverage formulation (butterfly pea flowers and spice components) were subjected to extraction prior to analysis. For this purpose, approximately 2.00 ± 0.01 g of sample was mixed with 5 mL of extraction solvent comprising methanol–water mixtures (3:7, 5:5, and 7:3 v/v). The mixtures were treated in an ultrasonic bath at 30°C for 15 min to enhance extraction efficiency. The samples were subsequently centrifuged at 2,700×g for 10 min at 4 ± 1°C and supernatant was collected. This procedure was repeated twice to ensure complete extraction. The combined extracts were filtered through membrane filter paper, transferred into centrifuge tubes, and stored at –20 ± 2°C for further analyses. The obtained extracts were used for spectrophotometric determination of TPC, TAC, and TMA content (Kamiloglu *et al.*, 2016).

Total phenolic content analysis

Total phenolic content was determined using the modified Folin–Ciocalteu method described by Kamiloglu *et al.* (2016). In this method, the extract was reacted with Folin–Ciocalteu reagent, followed by the addition of Na_2CO_3 solution, and the mixture was incubated in the dark at room temperature for 90 min for color development. Absorbance of the resulting solution was measured at 725 nm using a spectrophotometer. A calibration curve was prepared using gallic acid standards within the concentration range of 10–800 ppm, and the results were expressed as mg gallic acid equivalent (GAE) per 100 g dry matter (dm) (coefficient of determination, $R^2 = 0.9991$).

Total antioxidant capacity analysis

The antioxidant capacity of butterfly pea beverage extracts was evaluated using two different assays: DPPH and FRAP.

DPPH assay: The DPPH radical scavenging activity was determined according to the method described by Kumaran and Karunakaran (2006). In this assay, the extract was mixed with DPPH radical solution and incubated in the dark for 30 min for occurrence of radical scavenging reaction. After incubation, decrease in absorbance was measured at 517 nm using a spectrophotometer. A Trolox calibration curve prepared with different concentrations of Trolox (10–800 ppm) was used for quantification, and the results were expressed as µmol trolox equivalent (TE) per g dm (coefficient of determination, $R^2 = 0.9997$).

FRAP assay: The FRAP assay was carried out according to the method described by Kamiloglu and Capanoglu (2014). In this method, the extract was reacted with freshly prepared FRAP reagent consisting of acetate buffer, TPTZ (2,4,6-tris(2-pyridyl)-s-triazine) solution, and ferric chloride ($FeCl_3$). The mixture was incubated for a short period, and absorbance of the resulting blue-colored complex was measured at 593 nm. TAC was calculated using the Trolox calibration curve and expressed as µmol TE per g dm (coefficient of determination, $R^2 = 0.9934$).

Total monomeric anthocyanin analysis

Total monomeric anthocyanin content was determined using the pH differential method described by Lee *et al.* (2005). In this method, aliquots of the sample were mixed with potassium chloride (KCl) buffer (pH 1.0) and sodium acetate buffer (pH 4.5) in separate tubes, and absorbance was measured at 512 nm and 700 nm using a spectrophotometer. The difference in absorbance between two pH conditions was used to calculate TMA content according

to standard equation (3), and the results were expressed as cyanidin-3-glucoside equivalents:

$$TMA\left(\frac{mg}{kg}\right) = A \times MW \times DF \times (1{,}000 / \varepsilon \times L) \quad (3)$$

where:

$$A = (A\lambda_{512} - \lambda_{700})pH\ 1.0 - (A\lambda_{512} - \lambda_{700})pH\ 4.5 \quad (4)$$

MW = dominant anthocyanin in sample molecular weight

DF = dilution factor,

ε = absorbance coefficient and

L = layer thickness of spectrophotometer cuvettes (cm).

In vitro gastrointestinal digestion

In vitro gastrointestinal digestion of butterfly pea beverage samples was carried out according to the standardized static digestion method described by Minekus *et al.* (2014), which simulates gastric and intestinal digestion under controlled laboratory conditions and is widely used to evaluate the bioaccessibility of food components. Simulated gastric fluid (SGF) and simulated intestinal fluid (SIF) were prepared according to the INFOGEST (Improving Health Properties of Food by Sharing Our Knowledge on the Digestive Process) consensus protocol using electrolyte stock solutions containing KCl, KH_2PO_4, $NaHCO_3$, NaCl, $MgCl_2{\cdot}6H_2O$, $(NH_4)_2CO_3$, and calcium chloride ($CaCl_2{\cdot}2H_2O$). Gastric digestion was performed using porcine pepsin, whereas intestinal digestion was conducted using pancreatin and bile salts prepared according to the INFOGEST recommendations. The digestion media were adjusted to the target pH values specified by the protocol and all digestion steps were conducted under physiologically relevant conditions.

To simulate gastric digestion, beverage samples were mixed with simulated gastric fluid containing porcine pepsin and $CaCl_2{\cdot}2H_2O$, and the pH was adjusted to 3.0 using hydrochloric acid (HCl). The mixture was incubated at 37°C in a shaking water bath for 2 h. Subsequently, the intestinal digestion phase was initiated by mixing gastric digesta with simulated intestinal fluid containing pancreatin and bile salts. The pH of the mixture was adjusted to 7.0 using NaOH, and the digestion was continued at 37°C for an additional 2 h. At the end of digestion, the samples were centrifuged at 3,500 rpm for 10 min to separate insoluble particles, and the supernatant was collected after filtration. Both gastric and intestinal digested fractions were stored at −20 ± 2°C for further analyses.

Artificial neural network modeling

The experimental dataset consisted of 10 beverage formulations as mentioned above (C, C-PG, RO, RO-PG, FE, FE-PG, CA, CA-PG, MI, and MI-PG), three digestion stages (undigested, gastric digested, and intestinal digested), and three analytical replicates for each condition, resulting in a total of 90 observations. For each observation, TMA, TAC (determined by DPPH and FRAP assays), TPC, color parameters (L*, a*, b*, C*, and h°), pH, and total soluble solids (TSS) were recorded. In addition, the *in vitro* bioaccessibility responses obtained after gastric and intestinal digestion were incorporated into the modeling framework to evaluate digestion-induced changes in beverage quality. No explicit weighting factors were assigned to functional and color-related parameters during the optimization procedure. Instead, all selected responses were simultaneously incorporated into the scoring system to identify formulations exhibiting the most balanced overall performance. This approach was adopted to ensure that neither functional quality nor visual characteristics were disproportionately favored during formulation ranking.

Prior to ANN development, the dataset was reorganized into long-format structure, in which each row represented one unique sample × digestion stage × replicate combination. This arrangement enabled simultaneous modeling of formulation effects, digestion stage, and analytical variability within a unified dataset. Categorical descriptors were encoded numerically for ANN processing. Sample identity was represented by SampleCode, base raw material by BaseCode, and the presence of PG by a binary variable (0 = absent, and 1 = present). Digestion stage was encoded as StageCode (1 = undigested, 2 = gastric, 3 = intestinal).

The ANN analysis was performed using MATLAB Online (MathWorks Inc., Natick, MA, USA) with neural network Toolbox. A feed-forward multilayer perceptron (MLP) architecture trained by back propagation was employed to construct predictive models. The final input layer comprised 11 variables: SampleCode, BaseCode, PG, StageCode, L*, a*, b*, C*, h°, pH, and °Brix. The output layer comprised four target responses: TMA, DPPH, FRAP, and TPC. The general structure of the optimized ANN architecture is presented in Figure 3.

Prior to model training, all input and output variables were normalized to the range of −1–+1 using the

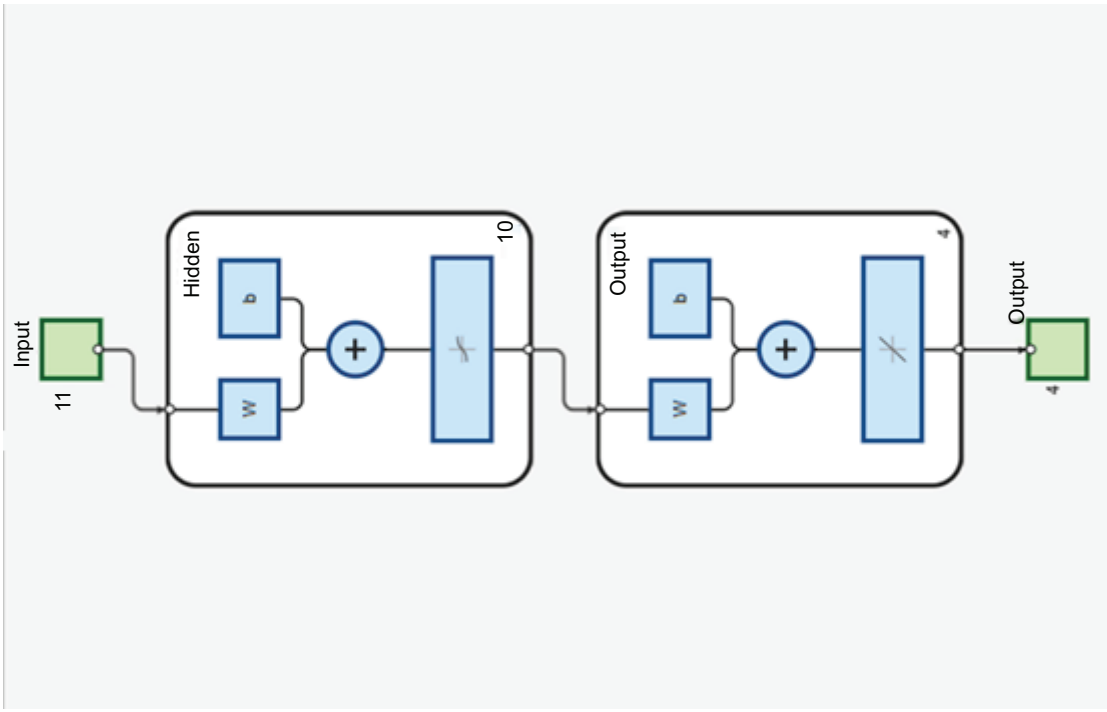

Figure 3. Artificial neural network architecture.

min–max normalization procedure implemented by the mapminmax function in MATLAB. This preprocessing step was applied to remove the influence of different measurement scales, improve numerical stability, and enhance convergence behavior during training.

The available dataset was randomly divided into training (70%), validation (15%), and testing (15%) subsets. The training subset was used to iteratively update network weights during learning; the validation subset was used to monitor prediction error and prevent overfitting through early stopping, and the testing subset was used to evaluate the predictive performance of the final model on unseen data.

The training process was performed using the Levenberg–Marquardt (LM) backpropagation algorithm (trainlm), which is widely preferred for nonlinear regression problems because of its fast convergence and strong predictive capability (Inyang and Obunikut, 2022). To determine the most appropriate network complexity, different hidden neuron numbers (5, 8, 10, 12, and 15) were evaluated using a single hidden layer. As shown in Table 1, the ANN model containing 10 hidden neurons provided the highest correlation coefficient and one of the lowest MSE values. Therefore, the 11–10–4 architecture was selected as the optimum network topology for subsequent prediction and optimization analyses.

Model performance was assessed using the correlation coefficient (R) and mean square error (MSE) calculated between predicted and experimental values. The network architecture providing the highest correlation coefficient together with a low prediction error was selected as the final model. Based on these criteria, the ANN containing one hidden layer with 10 neurons (11–10–4 topology) was selected for subsequent analyses.

The training behavior and validation performance of the optimized model are illustrated in Figure 4, where the reduction of error during successive epochs and the use of the best validation point as an early stopping criterion can be observed. This procedure ensured that the selected ANN model achieved high predictive accuracy while maintaining generalization ability.

After model development, predicted response values were integrated into a multi-response optimization framework to identify the most desirable beverage formulation. A composite desirability score was calculated by combining predicted TMA, DPPH, FRAP, and TPC values with a color quality score. For functional responses, higher predicted values were considered more desirable. For color optimization, preference was given to samples exhibiting vivid blue appearance, characterized by more negative b* values, higher chroma (C*), appropriate lightness (L*), and

negative a* values. All desirability components were scaled between 0 and 1 and combined using weighted summation. Equal weighting was assigned to functional and color criteria in order to achieve a balanced optimization strategy.

The inclusion of color parameters (L*, a*, b*, C*, and h°) as ANN inputs was based on their practical relevance as rapidly measurable quality indicators that may reflect compositional changes occurring in anthocyanin-rich beverage systems. Previous studies have demonstrated significant associations between color coordinates and anthocyanin content, phenolic composition, and antioxidant activity in plant-based foods. Therefore, color parameters were incorporated as complementary predictors with pH, soluble solids content, formulation descriptors, and digestion stage to improve the overall predictive capability of the model. Rather than representing target variables, these measurements were treated as experimentally observable quality descriptors that may contain useful information regarding the biochemical status of the beverage matrix (Muzolf-Panek and Waśkiewicz, 2022).

The trained ANN model was subsequently used to rank beverage samples and digestion-stage combinations according to their overall desirability scores, and the highest-scoring conditions were identified as the optimum formulations. This integrated modeling approach enabled simultaneous evaluation of functional quality, digestion-related bioaccessibility, and visual quality, thereby providing a robust decision-support tool for the development of optimized butterfly pea beverage formulations.

Table 1. Comparison of ANN architectures with different hidden neuron numbers for prediction of TMA, DPPH, FRAP, and TPC.

Neuron	Correlation coefficient (R)	MSE
5	0.93738	0.04438
8	0.90653	0.06526
10	0.96952	0.02189
12	0.96846	0.02233
15	0.96911	0.02189

Notes: TMA: total monomeric anthocyanin; ANN: artificial neural network; FRAP: ferric reducing antioxidant power; TPC: total phenolic content; DPPH: 2,2-diphenyl-1-picrylhydrazyl; MSE: mean square error.

Statistical analysis

All analyses were performed in triplicate. The obtained data were analyzed using the SPSS statistical software (version 23.0, SPSS Inc., Chicago, IL, USA). Statistical differences among samples were evaluated using one-way analysis of variance (ANOVA), followed by Tukey's multiple comparison test, and $P < 0.05$ was considered statistically significant. Calibration curves and coefficient of determination/correlation coefficient (R^2/R) were calculated using Microsoft Excel 2011 (Microsoft Corporation, Redmond, WA, USA). In addition, multivariate statistical analyses, including principal component analysis (PCA) and hierarchical cluster analysis (HCA) were conducted using Minitab version 21.0. PCA was used to identify patterns and relationships between physicochemical and bioactive parameters, whereas HCA was applied to classify beverage samples according to their similarity levels. Pearson correlation analysis was performed to evaluate relationships among physicochemical, color, phenolic, anthocyanin, and

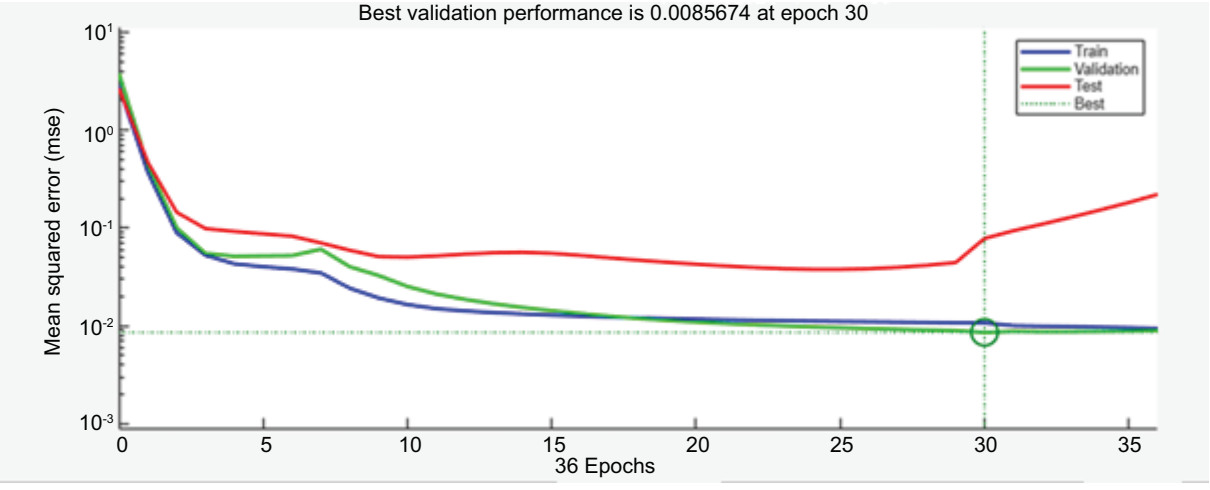

Figure 4. Training and validation error behavior during ANN model development and early-stopping procedure.

antioxidant parameters, with statistical significance set at $p < 0.05$.

Results and Discussion

pH, °Brix, and color values

If both pH and °Brix results obtained within the scope of this study were evaluated, statistically significant differences ($P < 0.05$) were found among the samples (Table 2). In terms of pH, the highest value was determined in the control sample, C (6.02), while the lowest value was observed in the RO-PG sample (5.07). In general, all PG-added samples (C-PG, RO-PG, FE-PG, CA-PG, and MI-PG) exhibited a clear decrease in pH values, compared to their plain counterparts. This situation can be explained by increase in the total acidity of the beverage because of the presence of organic acids, phenolic compounds, and sulfur-containing components in PG extracts. In particular, allicin derivatives found in garlic, and phenolic acids found in pepper, are thought to decrease pH by increasing the proton concentration of the medium. Indeed, compounds with a thiosulfinate structure, such as allicin, have been reported to possess high reactivity and to undergo protonation and chemical transformation reactions depending on changes in pH (García *et al.*, 2023).

In case TSS values were examined, the lowest value was found in the control sample (0.50 °Brix), while the highest value was determined in the FE-PG sample (1.20 °Brix). Increase in TSS values in all PG-containing samples indicates that spice extracts increased the soluble dry matter content of the beverages. This increase is not only

Table 2. pH, °Brix, and color values of beverage samples.

Sample	pH	°Brix
C	6.02 ± 0.01^{a}	0.50 ± 0.00^{g}
C-PG	5.65 ± 0.03^{d}	0.60 ± 0.01^{f}
RO	5.12 ± 0.02^{h}	0.70 ± 0.00^{e}
RO-PG	5.07 ± 0.01^{i}	0.90 ± 0.01^{c}
FE	5.36 ± 0.01^{g}	0.90 ± 0.01^{c}
FE-PG	5.11 ± 0.00^{h}	1.20 ± 0.00^{a}
CA	5.49 ± 0.02^{e}	0.80 ± 0.01^{d}
CA-PG	5.40 ± 0.01^{f}	1.00 ± 0.01^{b}
MI	5.96 ± 0.00^{b}	0.70 ± 0.01^{e}
MI-PG	5.78 ± 0.02^{c}	0.90 ± 0.00^{c}

	Color				
	L*	a*	b*	C*	h°
C	52.35 ± 0.05^{f}	–15.63 ± 0.01^{g}	–40.58 ± 0.01^{g}	38.52 ± 0.02^{a}	240.15 ± 0.12^{c}
C-PG	55.22 ± 0.03^{e}	–5.13 ± 0.01^{b}	–38.49 ± 0.02^{e}	37.13 ± 0.03^{b}	256.59 ± 0.16^{a}
RO	50.67 ± 0.07^{g}	–18.62 ± 0.04^{h}	–25.13 ± 0.03^{d}	26.78 ± 0.02^{g}	120.65 ± 0.09^{j}
RO-PG	45.12 ± 0.02^{i}	–9.40 ± 0.04^{d}	–23.10 ± 0.00^{c}	22.12 ± 0.00^{i}	162.18 ± 0.14^{g}
FE	80.25 ± 0.05^{a}	–5.94 ± 0.02^{c}	–45.96 ± 0.02^{j}	33.18 ± 0.01^{d}	236.28 ± 0.17^{d}
FE-PG	75.63 ± 0.08^{b}	–3.82 ± 0.01^{a}	–42.35 ± 0.03^{i}	30.96 ± 0.01^{f}	249.69 ± 0.05^{b}
CA	68.15 ± 0.01^{c}	–12.75 ± 0.03^{f}	–41.38 ± 0.03^{h}	23.16 ± 0.02^{h}	235.84 ± 0.04^{e}
CA-PG	60.42 ± 0.04^{d}	–10.82 ± 0.02^{e}	–39.50 ± 0.05^{f}	20.05 ± 0.05^{j}	210.23 ± 0.13^{f}
MI	48.53 ± 0.03^{h}	–20.35 ± 0.03^{i}	–16.39 ± 0.00^{b}	36.16 ± 0.01^{c}	123.16 ± 0.05^{i}
MI-PG	44.37 ± 0.02^{j}	–10.72 ± 0.01^{e}	–14.63 ± 0.01^{a}	31.03 ± 0.02^{e}	154.55 ± 0.11^{h}

Notes: Values are expressed as mean ± standard deviation (SD) (n = 3).
Mean values followed by different lowercase superscript alphabets within the same column indicate statistically significant differences at $P < 0.05$ according to Tukey's test.
h° = hue angle; C = butterfly pea control; C-PG = butterfly pea + pepper + garlic; RO = rosemary extract; RO-PG = rosemary + pepper + garlic; FE = fenugreek extract; FE-PG = fenugreek + pepper + garlic; CA = cardamom extract; CA-PG = cardamom + pepper + garlic; MI = mint extract; MI-PG = mint + pepper + garlic.

because of sugars but also soluble phenolics, organic acids, nonvolatile aromatic compounds, and mineral content. Previous studies have reported that TSS values reflect not only sugars but also organic acids, proteins, and other soluble components (Reis *et al.*, 2025). The higher TSS values observed particularly in FE-PG and CA-PG samples suggest that components such as fenugreek and cardamom have higher extractable solid content.

In the literature, the addition of different plant extracts to herbal infusions similarly affects pH and soluble solid content. In particular, in plant-based beverages, increasing extract concentration has been associated with a decrease in pH and an increase in TSS. Studies on butterfly pea (*C. ternatea*) tea have also indicated that the anthocyanins present in this beverage are highly sensitive to pH and an increase in acidic components alters the chemical equilibrium of the system (Hasanah *et al.*, 2023). Therefore, the addition of different plant extracts not only changes the pH value but also reshapes the chemical structure and functional properties of the beverage.

In case, the obtained results are evaluated with the literature, first, spice extracts contain water-soluble low molecular weight organic acids and phenolic compounds, and the transfer of these compounds into the medium directly leads to a decrease in pH. Second, these compounds are perceived as soluble solids in refractometric measurements, resulting in an increase in TSS values. Third, anthocyanins present in butterfly pea tea transform into different ionic forms depending on pH, and this transformation alters the chemical equilibrium of the system. Indeed, the addition of plant extracts to butterfly pea beverages decreases pH because of the chemical composition of plant components (Malçok *et al.*, 2025). In addition, anthocyanins have been shown to undergo structural transformations depending on pH, and these transformations directly affect the color and chemical properties of the solution (Hasanah *et al.*, 2023; Widyawati *et al.*, 2024).

In addition, the differences observed among plant extracts are attributed to the unique phytochemical profiles of each plant. For example, higher TSS values observed in fenugreek and cardamom samples are associated with their higher extractable polysaccharide and phenolic content, whereas lower pH values in PG-containing samples are explained by their stronger acidic character. This clearly demonstrates that plant components used in functional beverage formulations not only influence sensory properties but also significantly modulate physicochemical characteristics. Similarly, spices are rich in phenolic acids and flavonoids, and these compounds can easily be transferred into aqueous media, thereby affecting the chemical properties of food systems (Duque-Soto *et al.*, 2023). It is also reported that structural differences of phenolic compounds determine their solubility, reactivity, and interactions within the system, leading to different physicochemical outcomes depending on the plant source (Alara *et al.*, 2021).

The extraction conditions applied in this study were selected to reflect realistic beverage preparation practices while ensuring consistency among formulations. The infusion temperatures, extraction times, and plant-to-water ratios used are generally comparable to those employed during the preparation of herbal and functional beverages by consumers. Therefore, the physicochemical and functional properties reported here may provide a reasonable approximation of the characteristics that could be encountered under practical consumption conditions. Nevertheless, variations in domestic preparation practices, including brewing time, temperature, and ingredient concentration, may influence the final composition and bioactive profile of the beverages.

Color parameters showed statistically significant differences among beverage samples ($P < 0.05$). In terms of L*, the highest value was observed in the FE sample (80.25), whereas the lowest value was recorded in the MI-PG sample (44.37). This indicates that fenugreek extract imparted a lighter/brighter appearance to the beverage, whereas mint + PG combination resulted in a darker appearance. Similarly, PG addition decreased the L* value in all groups, compared to their corresponding plain samples (e.g., RO: 50.67 → RO-PG: 45.12; CA: 68.15 → CA-PG: 60.42; MI: 48.53 → MI-PG: 44.37) (Table 2). This trend can be explained by the increased light absorption and scattering caused by pigments and soluble solids transferred into the solution with the added extracts. Studies on butterfly pea tea have likewise reported that infusion conditions significantly affect L* values and that more intense extraction conditions lead to darker color formation (Hasanah *et al.*, 2023).

With respect to a* parameter, all samples exhibited negative values, indicating that all beverages were positioned on the green axis rather than the red axis. The lowest a* value was detected in the MI sample (–20.35), whereas the highest a* value was found in the FE-PG sample (–3.82). A larger absolute negative a* value indicates a stronger greenish component. The lower a* values observed in mint- and rosemary-containing samples may be related to the chlorophyll-like/greenish tonal contribution of these botanicals and their interactions with butterfly pea pigments. In contrast, with addition

of PG, a* values in most samples shifted closer to zero (0), suggesting that the relative contribution of green tones weakened or that the system shifted toward a more purple-blue balance.

The fact that all b* values were negative indicates, as expected, that the samples were positioned on the blue axis rather than the yellow axis. The lowest b* value was observed in the FE sample (–45.96), whereas the highest value was found in the MI-PG sample (–14.63). Since more negative b* values correspond to a more pronounced blue color, both FE and FE-PG represented the strongest blue tones. Ternatin-type anthocyanins in butterfly pea flowers exhibit pronounced pH sensitivity, with blue/anionic quinonoidal forms predominating under near-neutral conditions. Consequently, variations in b* values may reflect not only the color contribution of the extracts themselves but also pH-induced shifts in anthocyanin equilibria caused by the added botanical ingredients (Khoo *et al.*, 2017).

C* (chroma) values provide information on color saturation or vividness. The highest C* value was found in the control sample (38.52), followed by C-PG (37.13) and MI (36.16), whereas the lowest value was detected in the CA-PG sample (20.05). This result suggests that the control sample exhibited a purer and more saturated butterfly pea blue, while some addition of spice rendered dull color. Reduced C* values in cardamom- and rosemary-containing samples may be associated with increased turbidity, color dilution effects, or potential interactions between anthocyanins and other phenolic constituents present in botanical extracts. However, since phenomenon of co-pigmentation was not evaluated directly in the present study, such an interaction must be regarded as a plausible hypothesis rather than a confirmed mechanism. Literature has reported that C* values in butterfly pea systems vary significantly depending on extraction conditions and matrix composition, and that even when pigment oncentration increases, the color does not always appear more vivid (Zor *et al.*, 2023).

Hue (h°) values are particularly important in the interpretation of results. The h° value of the control sample was 240.15, corresponding to a typical blue region. C-PG (256.59) and FE-PG (249.69) also remained within the blue-purple axis. In contrast, the markedly lower h° values of MI (123.16) and RO (120.65) indicate that these samples deviated from the classical butterfly pea blue and shifted toward different hue compositions. In the CIELAB system, h° values of approximately 240–270° correspond to blue, around 270° to a blue-purple transition, and lower values indicate greenish or shifted tones. Therefore, especially in mint- and rosemary-containing samples, the dominant butterfly pea blue appears to have been influenced by the presence of botanical pigments and changes in the surrounding phenolic matrix, although the specific mechanisms responsible for these shifts were not investigated directly (Maneechot *et al.*, 2023).

In case, plain and PG-added samples were compared together, addition of PG generally caused simultaneous changes in L*, a*, b*, C*, and h° parameters. In other words, PG addition not only lowered pH but also reshaped hue and color saturation. In particular, in the transition from C to C-PG, the increase in a* from –15.63 to –5.13 and in h° from 240.15 to 256.59 indicates that the color was rebalanced along the blue-purple axis. In RO/RO-PG and CA/CA-PG pairs, addition of PG further reduced L* and C*, resulting in a darker and less saturated appearance. This finding suggests that the added extracts did not merely contribute pigments but they also altered optical properties through turbidity, increased solids, and phenolic interactions.

If studies on butterfly pea tea in the literature are examined, it is determined that color parameters exhibit considerable variability. For example, in a study conducted on infusion tea samples obtained from butterfly pea flowers, beverages were prepared using different brewing temperatures (70°C, 80°C, and 90°C) and durations (9, 18, and 27 min). L*, a*, b*, C*, and h° values were reported to range between 37.45–38.27, 2.45–4.00, 2.84–4.26, 3.78–5.88, and 42.37–49.37, respectively. According to the color analysis results, L*, a*, b*, C*, and h° values were significantly affected by brewing conditions; particularly, higher temperatures and longer extraction periods decreased L* values (indicating darker color formation) and led to more negative b* values (indicating more intense blue color) (Zor *et al.*, 2023).

In studies investigating the color properties of infusions obtained from butterfly pea flowers, generally hot water extraction (80–100°C, 10–20 min) is applied. In these studies, L* values were reported to vary approximately 40–80, while b* values were distinctly negative, ranging from –15 to –45. It was emphasized that under more intense extraction conditions, L* values decreased (darker color), whereas b* values became more negative (more intense blue tone). This phenomenon was associated with increased anthocyanin concentration (Aljumayi *et al.*, 2025).

In another study, butterfly pea extract was evaluated under different pH conditions, and it was demonstrated that color parameters varied within a wide range. Particularly, within the pH range of 4–7, the system exhibited blue-purple tones, and the hue angle was reported to be approximately 230–270°. At lower pH

values, a shift toward red tones was observed, while at higher pH values, transitions toward greenish tones were reported (Handayani *et al.*, 2024).

In a study where beverages were produced using butterfly pea and purple basil through conventional infusion and ultrasound-assisted infusion for 3–7 min, L* values were reported as 44.50/68.10, a* values as –18.49/–6.23, b* values as –41.58/–16.53, C* values as 19.18/43.20, and h° values as 237.55°/258.78°. This study demonstrated that the color values of butterfly pea infusions could vary significantly depending on infusion conditions and the composition of added plant materials (Malçok *et al.*, 2025).

In a similar study (Gomez *et al.*, 2022), color analysis was performed on butterfly pea flower extract. As a result of this study, L*, a*, b*, C*, and h° values of the extracts were determined in the range of 18.09–49.24; 36.78–46.90; -38.02–-63.25; 52.90–78.74; and 306.56°–319.44°, respectively. Also, in another study (Hariadi *et al.*, 2018), the color values of butterfly pea flower extracts were found as L*: 51.72, a*: 23.50, and b*: 8.42.

In addition, in a study where purple basil was added to butterfly pea beverage, the second botanical matrix was reported to alter the pH of beverage and, consequently, its color characteristics; this supports the view that spice extracts in the present study similarly modulated the butterfly pea pigment system (Fu *et al.*, 2021).

Compared with the literature, color parameters in butterfly pea beverages are known to be highly sensitive to infusion temperature, time, pH, and the accompanying botanical matrix. A study on *Clitoria ternatea* tea reported that infusion temperature and time caused significant changes, particularly in a*, b*, C*, and h° values, and that increasing extraction intensity markedly shifted color coordinates (Zor *et al.*, 2023).

From a food chemistry perspective, these differences are mainly attributable to the pH-dependent structural transformations of ternatin-type polyacylated anthocyanins present in butterfly pea flowers. Under highly acidic conditions, the flavylium form is favored, whereas neutral and anionic quinonoidal base forms become dominant with increase in pH. These transformations are well known to affect hue. In addition, phenolic acids and other secondary metabolites derived from spice extracts may have contributed to the observed color differences through modifications of beverage matrix and pigment environment. Possible co-pigmentation or pigment–phenolic interactions cannot be excluded; however, these mechanisms were not directly measured in the present study and therefore remain speculative. Moreover, soluble solids and colloidal components transferred from the extracts may have increased light scattering and thereby influenced L* and C* values. Consequently, the observed color differences should be interpreted as the combined outcome of changes in pH, anthocyanin transformations, effects of matrix, and optical scattering phenomena rather than as direct evidence of specific co-pigmentation mechanisms (Hasanah *et al.*, 2023).

TPC and *in vitro* bioaccessibility

Undigested samples exhibited TPC values ranging from 756.30 to 5299.33 mg GAE/100 g, and statistically significant differences were observed among samples ($P < 0.05$) (Table 3). The highest TPC value was determined in the MI-PG sample (5,299.33 ± 246.00 mg GAE/100 g), followed by MI (4,270.41 ± 960.50 mg GAE/100 g) and RO-PG (3,816.94 ± 152.46 mg GAE/100 g), whereas the lowest value was observed in the control (C) sample (756.30 ± 146.08 mg GAE/100 g). This ranking suggests that the diversity of phenolic pool and differences in extractability (phenolic acids, flavonoids, phenolic diterpenes, etc.) in plant extracts can significantly modulate the measured TPC values of the beverage system. For instance, rosmarinic acid is one of the dominant phenolics in Mentha species and shows a strong correlation with total phenolic/antioxidant response; this provides a biochemical basis for the high TPC profile of MI and MI-PG samples (Cirlini *et al.*, 2016).

The strong antioxidant character of phenolic diterpenes, such as carnosic acid and carnosol in rosemary, and their ability to suppress oxidative processes in food systems, is consistent with the relatively high TPC values observed in RO and RO-PG samples. Similarly, the phenolic profile and antioxidant properties of fenugreek (*Trigonella foenum-graecum*) seed extracts confirmed by ultra performance liquid chromatography–mass spectrometry (UPLC-MS) can explain the high TPC values of FE/FE-PG samples (Kenny *et al.*, 2013). In garlic, the presence of allicin and other organosulfur compounds, and in pepper, the presence of phenolics and capsaicinoids, mechanistically support the increase in pre-digestion TPC values in some PG-added samples (e.g., increases in C→C-PG and RO→RO-PG) (Borlinghaus *et al.*, 2014).

In butterfly pea-based beverages, TPC content varies widely depending on the form of raw material, extraction method, and beverage formulation. Recent studies have demonstrated that these beverages contain considerable amounts of phenolic compounds and possess functional beverage potential. For example, Nafisah *et al.* (2024)

Table 3. Total phenolic content and *in vitro* bioaccessibility of beverage samples.

Sample	Undigested (mg GAE/100 g)	*In vitro* gastric digested (mg GAE/100 g)	*In vitro* intestinal digested (mg GAE/100 g)
C	756.30 ± 146.08^{e,C}	943.16 ± 45.61^{d,B}	3,068.31 ± 962.12^{d,A}
C-PG	998.42 ± 70.80^{e,B}	497.03 ± 171.59^{d,C}	2,653.76 ± 382.56^{d,A}
RO	2,752.26 ± 1,595.16^{d,B}	2,396.12 ± 1,458.33^{c,C}	7,036.43 ± 2,981.14^{c,A}
RO-PG	3,816.94 ± 152.46^{c,B}	2,782.79 ± 1,015.36^{c,C}	7,163.93 ± 1,112.72^{c,A}
FE	3,720.53 ± 507.34^{c,B}	2,967.80 ± 888.88^{c,C}	8,848.69 ± 98.53^{b,A}
FE-PG	3,573.77 ± 161.30^{c,B}	3,039.81 ± 770.14^{c,C}	7,768.41 ± 1,436.23^{b,A}
CA	3,076.89 ± 679.30^{d,C}	3,446.14 ± 1,871.11^{b,B}	11,028.69 ± 4,616.18^{a,A}
CA-PG	3,227.75 ± 661.07^{d,B}	2,961.94 ± 164.66^{c,C}	12,813.69 ± 2,776.49^{a,A}
MI	4,270.41 ± 960.50^{b,C}	4,627.35 ± 1,094.77^{a,B}	9,542.34 ± 4,544.64^{b,A}
MI-PG	5,299.33 ± 246.00^{a,B}	5,217.24 ± 909.70^{a,C}	9,719.49 ± 2,240.64^{b,A}

Notes: Values are expressed as mean ± standard deviation (SD; n = 3).
Different lowercase superscript alphabets within the same column and different uppercase superscript alphabets within the same row indicate statistically significant differences ($P < 0.05$) according to Tukey's test.
C = butterfly pea control; C-PG = butterfly pea + pepper + garlic; RO = rosemary extract; RO-PG = rosemary + pepper + garlic; FE = fenugreek extract; FE-PG = fenugreek + pepper + garlic; CA = cardamom extract; CA-PG = cardamom + pepper + garlic; MI = mint extract; MI-PG = mint + pepper + garlic.

reported that the TPC of a kombucha-type fermented beverage prepared using butterfly pea flowers was 124.46 mg GAE/L. In the same study, this value was reported as 162.35 mg GAE/L in traditional green tea kombucha, indicating that butterfly pea-based beverages have a considerable TPC, although lower than tea-based systems.

Similarly, in a study conducted by Wahyanto and Agustini (2024), a functional beverage was developed by enriching green tea kombucha with butterfly pea flower extract. It was reported that the addition of extract increased TPC and TFC, and anthocyanin-derived phenolics contributed significantly to the TAC of the beverage.

In another study investigating the combination of butterfly pea flower with different plant materials (beverage formulation containing 30% butterfly pea extract), TPC was determined as 322.67 mg GAE/L. This result indicates that plant mixtures can significantly enhance phenolic content and create a synergistic effect (Anggraini *et al.*, 2022).

In terms of raw material, Kuswandari *et al.* (2022) reported that TPC of butterfly pea flower extract ranged between 1,924.96 mg GAE/100 g and 2,459.94 mg GAE/100 g. These high values indicate that phenolic compounds are diluted during beverage production, although the raw material itself is a rich phenolic source. Moreover, in a study conducted using different extraction solvents (Kurniawati *et al.*, 2024), the TPC of butterfly pea flower extracts ranged between 78.63 mg GAE/100 g and 93.91 mg GAE/100 g extract, with 70% ethanol providing the highest phenolic yield. This finding demonstrates that the extraction method directly affects phenolic content in beverage production. Finally, in kombucha-like beverages developed using butterfly pea flowers, it is reported that phenolic and antioxidant compounds increase during fermentation and functional properties improve along with organic acid formation. This indicates that fermentation is an important process that enhances both bioavailability and total amount of phenolic compounds (Aksornsri *et al.*, 2023).

In all formulations, TPC values increased substantially after intestinal digestion, although gastric digestion responses varied among samples. Undigested TPC values ranged from 756.30 mg GAE/100 g in the control sample to 5,299.33 mg GAE/100 g in MI-PG. Following intestinal digestion, TPC increased to 2,653.76–12,813.69 mg GAE/100 g, representing increase of approximately 83–306%, relative to the undigested state. Maximum intestinal TPC values were observed in CA-PG (12,813.69 mg GAE/100 g), CA (11,028.69 mg GAE/100 g), MI-PG (9,719.49 mg GAE/100 g), and MI (9,542.34 mg GAE/100 g). In contrast, gastric digestion produced more variable effects, with some formulations showing moderate increase (e.g., CA and MI), while others exhibited reduction. Overall, the marked enhancement of TPC after intestinal digestion suggests extensive release of phenolic

compounds from the beverage matrix under simulated gastrointestinal conditions.

These results indicate that while limited increase/decrease was observed in the gastric phase in most samples, a significant increase in TPC was observed in all samples in the intestinal phase (e.g., +305.7% in control; and +297.0% in CA-PG).

Similar findings are reported in the literature. For example, Malçok *et al.* (2025) reported that TPC values in butterfly pea tea and butterfly pea tea + purple basil beverages ranged from 9.30–70.78 mg GAE/100 g in the undigested state, increased to 286.83–463.55 mg GAE/100 g in the gastric phase, and further increased to 855.12–1,039.22 mg GAE/100 g in the intestinal phase. In another study where only infusion parameters were varied, TPC in butterfly pea tea was reported to range between 795.78 mg GAE/L and 1,000.68 mg GAE/L, and it was shown that increase in both temperature/time increased TPC, supporting that extraction intensity determines phenolic output in plant-based beverages (Zor *et al.*, 2023).

In a study conducted on a phenolic-rich plant by-product matrix, it was determined that TPC increased throughout digestion in the order of oral < gastric < intestinal, with approximately a 2.4-fold increase from gastric to intestinal phase. This increase was attributed to pancreatin, bile salts, and neutral pH conditions enhancing the release of phenolics from the matrix (Pinto *et al.*, 2023). Similarly, in a study on fermented *Aloe vera* beverages, digestion significantly increased TPC values, particularly in the intestinal phase where phenolics and cinnamic acid derivatives were released, leading to an increase in TAC.

In legume-based samples, TPC generally increased during digestion and reached maximum values in the intestinal phase. For example, in some samples, the intestinal phase TPC reached 4.76 mg GAE/g, and this increase was attributed to the release of bound phenolics (Li *et al.*, 2022). These findings support the general increasing trend observed in all samples during the intestinal phase in the present study.

In the present study, the decrease observed in some samples, such as C-PG, during the gastric phase is also consistent with literature findings. For instance, in a study conducted on eight different fruit juices, TPC bioaccessibility ranged as 13.52–26.49%, and a decrease was observed in some samples during the intestinal phase (Mihaylova *et al.*, 2021). The higher TPC values observed in the intestinal phase, compared to the gastric phase, can be explained by (i) increased solubility of cell wall/complex structures because of increased pH and ionic strength in the small intestine, (ii) weakening of matrix-bioactive interactions by pancreatic enzymes and bile salts, leading to increased 'releasable' phenolic fraction, and (iii) hydrolysis/transformation of some phenolic conjugates, resulting in increased measurable reducing capacity. These processes may promote the release of phenolics that were previously entrapped within the food matrix or associated with macromolecules, thereby increasing their extractability and measurable antioxidant activity. Indeed, Minekus/INFOGEST digestion conditions provide a physiological simulation that can trigger such release and transformations (Minekus *et al.*, 2014).

Similarly, studies on grape polyphenols demonstrate that TPC and antioxidant responses may change across both gastric and intestinal phases, with the extent of release and transformation depending on the food matrix (Tagliazucchi *et al.*, 2010). It should be noted that the INFOGEST static *in vitro* digestion model provides an estimation of bioaccessibility under standardized gastrointestinal conditions but does not fully replicate the complexity of human digestion. Factors such as individual physiological variability, absorption processes, intestinal metabolism, microbiota activity, and systemic distribution are not represented in the model. Therefore, the observed increase in TPC and TAC should be interpreted as indicators of potential bioaccessibility rather than actual *in vivo* bioavailability (Zhou *et al.*, 2023).

However, the sharp increase measured by Folin–Ciocalteu in the intestinal phase cannot be entirely attributed to phenolic release. Because Folin reagent can also react with thiols, proteins, and various reducing substances, digestive enzymes and digestion medium components (especially proteins/peptides and some reducing species) may increase measured TPC values (Everette *et al.*, 2010). Moreover, the formulation contained garlic and spice ingredients, which are known to provide sulfur-containing compounds and other reducing substances that may partially contribute to the Folin–Ciocalteu response. Therefore, the elevated intestinal-phase TPC values probably reflect both enhanced release of phenolic compounds and contribution of non-phenolic reducing constituents liberated during digestion. Similarly, studies reporting increased TPC during simulated gastrointestinal digestion attribute this increase to both release/enzyme effects and methodological/matrix effects (Bouayed *et al.*, 2011).

Total antioxidant capacity and *in vitro* bioaccessibility

In undigested samples, TAC values determined by DPPH were found to be in the range of 237.54–1,799.48 μmol trolox/g dm (Table 4). The highest

Table 4. Total antioxidant capacity and *in vitro* bioaccessibility of beverage samples.

DPPH (µmol trolox/g dm)			
Sample	**Undigested**	***In vitro* gastric digested**	***In vitro* intestinal digested**
C	237.54 ± 4.97^{f,B}	415.90 ± 132.41^{e,A}	176.13 ± 108.66^{f,C}
C-PG	251.01 ± 13.22^{f,B}	223.45 ± 16.63^{f,C}	497.45 ± 166.80^{e,A}
RO	957.01 ± 14.10^{d,B}	778.12 ± 100.09^{d,C}	1,300.87 ± 135.57^{b,A}
RO-PG	965.44 ± 13.96^{d,B}	881.62 ± 56.57^{d,C}	1,324.38 ± 153.64^{b,A}
FE	1,006.99 ± 21.28^{c,d,B}	997.05 ± 142.41^{c,B}	633.63 ± 58.27^{d,A}
FE-PG	1,092.85 ± 5.38^{c,B}	1,025.96 ± 91.43^{c,C}	1,204.59 ± 131.44^{c,A}
CA	660.88 ± 120.55^{e,C}	1,276.81 ± 122.49^{b,B}	1,455.46 ± 188.77^{a,A}
CA-PG	861.53 ± 61.23^{d,C}	1,406.34 ± 231.23^{a,B}	1,227.17 ± 100.92^{c,A}
MI	1,679.51 ± 103.87^{b,A}	1,200.00 ± 415.44^{b,B}	1,052.25 ± 156.50^{d,C}
MI-PG	1,799.48 ± 0.00^{a,A}	1,160.86 ± 136.44^{b,B}	1,224.25 ± 96.42^{c,C}
FRAP (µmol trolox/g dm)			
Sample	**Undigested**	***In vitro* gastric digested**	***In vitro* intestinal digested**
C	161.80 ± 6.33^{f,B}	1,234.86 ± 39.32^{a,A}	121.68 ± 15.43^{f,C}
C-PG	198.57 ± 13.33^{f,A}	171.47 ± 34.22^{f,B}	148.75 ± 18.25^{f,C}
RO	739.22 ± 34.94^{d,A}	562.92 ± 25.13^{d,B}	494.24 ± 25.90^{d,C}
RO-PG	749.57 ± 2.83^{d,A}	536.27 ± 78.49^{d,B}	451.70 ± 43.95^{d,C}
FE	839.32 ± 23.39^{c,A}	516.48 ± 35.89^{d,B}	512.00 ± 3.66^{c,C}
FE-PG	866.38 ± 7.79^{c,A}	653.46 ± 70.37^{c,B}	492.97 ± 38.17^{d,C}
CA	703.67 ± 75.00^{e,A}	451.83 ± 71.60^{e,B}	451.54 ± 97.60^{d,C}
CA-PG	718.38 ± 48.35^{e,B}	713.01 ± 130.02^{c,A}	446.89 ± 19.92^{d,C}
MI	1,114.53 ± 53.01^{b,A}	769.99 ± 50.48^{b,B}	524.03 ± 18.42^{c,C}
MI-PG	1,081.94 ± 18.92^{a,A}	704.57 ± 68.54^{c,B}	526.97 ± 45.41^{c,C}

Notes: Values are expressed as mean ± standard deviation (SD; n = 3).
Different lowercase superscript alphabets within the same column and different uppercase superscript alphabets within the same row indicate statistically significant differences ($P < 0.05$) according to Tukey's test.
C = butterfly pea control; C-PG = butterfly pea + pepper + garlic; RO = rosemary extract; RO-PG = rosemary + pepper + garlic; FE = fenugreek extract; FE-PG = fenugreek + pepper + garlic; CA = cardamom extract; CA-PG = cardamom + pepper + garlic; MI = mint extract; MI-PG = mint + pepper + garlic.

values were observed in MI-PG (1,799.48 ± 0.00 µmol trolox/g dm) and MI (1,679.51 ± 103.87 µmol trolox/g dm) samples, whereas the lowest value was determined in the control C (237.54 ± 4.97 µmol trolox/g dm) sample.

Accordingly, the high DPPH response observed in MI and MI-PG samples may be associated with the ability of mentha phenolics (particularly rosmarinic acid derivatives) and potentially co-extracted reducing compounds to donate electrons or hydrogen atoms to DPPH radical (Cirlini *et al.*, 2016).

Similarly, in another study examining blue flower beverages and variants enriched with purple basil, DPPH values in undigested samples ranged between 2.57 µmol trolox/g dm and 55.93 µmol trolox/g dm. These values were lower than those obtained in the present study and potentially reflect variations in formulation concentration, dry matter basis, and extraction intensity (Malçok *et al.*, 2025).

Similarly, in a study evaluating the effect of brewing temperature, DPPH results of blue tea infusions were expressed as IC_{50} values, and the lowest IC_{50} (~14,792 ppm) was obtained at 80°C. This further confirms that lower IC_{50} values correspond to higher TAC (Sitompul and Martati, 2025).

If considered in the context of fermented beverages, DPPH activity is reported to increase significantly during kombucha production. In particular, TAC was found to

increase approximately 2.88-fold by the end of fermentation, which was attributed to the biotransformation of phenolic compounds (Kim *et al.*, 2023).

Moreover, studies comparing extracts obtained using different solvents have demonstrated that DPPH results vary depending on the extraction method, with ethanol extracts generally exhibiting higher radical scavenging capacity (Nurhayati *et al.*, 2024).

In contrast to DPPH, FRAP analysis demonstrates 'reducing power' based on the color change resulting from the reduction of Fe(III)–TPTZ complex to Fe(II)–TPTZ complex under acidic conditions, thereby reflecting electron transfer capacity rather than direct radical scavenging activity. In the present study, FRAP values in undigested samples ranged from 161.80 to 1,114.53 µmol trolox/g dm, with the highest values observed in MI (1,114.53 ± 53.01 µmol trolox/g dm) and MI-PG (1,081.94 ± 18.92 µmol trolox/g dm) samples, and the lowest value in the control C (161.80 ± 6.33 µmol trolox/g dm) sample (Table 4). In the literature, FRAP values for blue tea infusions are reported in the range of 433.11–545.25 µM TE/mL, with increases observed at higher temperatures, including interactions with brewing time and particle size (Zor *et al.*, 2023).

Similarly, in the blue flower beverage enriched with purple basil, FRAP values in undigested samples ranged from 10.10 to 100.69 µmol trolox/g dm, and phase-dependent variations in FRAP responses following digestion were also reported (Malçok *et al.*, 2025).

In another study focusing on butterfly pea flower extract, FRAP values reached 1,093.83 µmol TE/L under extraction conditions at 60°C. It was further reported that increasing extraction time resulted in higher FRAP values, with maximum reducing power achieved at longer extraction duration (Duy *et al.*, 2020).

Furthermore, a review study highlighted that FRAP values of butterfly pea flower extracts vary over a wide range, with some studies reporting values as high as 0.33 mmol ascorbic acid equivalent/g and 13.3 millimoles of Trolox Equivalent per g (mM TEAC/g). These findings indicate that the plant possesses strong reducing capacity and that TPC and TMA content directly influence FRAP results (Jeyaraj *et al.*, 2021).

Consistent trends are also reported in functional food systems. For instance, in products enriched with butterfly pea extract, TAC (including FRAP) increased with rising extract concentration, which was closely associated with the presence of anthocyanins and phenolic compounds (Windarsih *et al.*, 2025).

Additionally, systematic evaluations have emphasized that butterfly pea flower is a potent antioxidant source because of its high anthocyanin content, and that these compounds contribute significantly to reducing capacity, thereby increasing FRAP values (Hasanah *et al.*, 2023). Accordingly, the relatively high FRAP values observed in blue tea and similar beverages are largely attributed to the presence of these pigments.

Overall, the literature indicates that FRAP values in blue tea and similar beverages vary widely depending on extraction temperature, time, solvent type, and composition of formulation. Nevertheless, systems rich in phenolic compounds and anthocyanins consistently exhibit elevated reducing capacity.

Furthermore, the observation that DPPH and FRAP results differ within the same samples is expected, as these assays are based on distinct chemical mechanisms and exhibit different sensitivities to the sample matrix (Schaich *et al.*, 2015).

Finally, the literature has consistently demonstrated that DPPH values in blue tea and similar beverages vary significantly depending on extraction methods, brewing conditions, and particularly, fermentation processes while generally indicating high antioxidant activity.

The DPPH antioxidant activity exhibited formulation-dependent changes during simulated gastrointestinal digestion. Undigested samples showed DPPH values ranging from 237.54 to 1,799.48 µmol Trolox/g dm, with MI and MI-PG exhibiting the highest initial antioxidant activities. Following intestinal digestion, DPPH values ranged between 176.13 µmol Trolox/g dm and 1,455.46 µmol Trolox/g dm. Maximum increase was obs erved in CA and C-PG, where intestinal digestion enhanced antioxidant activity by approximately 120% and 98%, respectively. In contrast, MI, MI-PG, and FE samples showed reduction in DPPH activity after digestion. Overall, the results indicate that the impact of gastrointestinal digestion on radical scavenging activity was highly formulation-dependent, reflecting differences in the release, transformation, and stability of antioxidant compounds within the beverage matrix.

These results indicate three critical points: (i) while an increase is observed in the gastric phase for some samples (C, CA, and CA-PG), a decrease is evident in others (RO and MI group); (ii) a clear increase is observed in the intestinal phase for CA and RO groups, whereas a marked decrease occurs in MI and FE samples; (iii) the phase response differs between PG-containing variants and non-PG variants of the same matrix (e.g., C-PG

shows a strong increase in the intestinal phase, i.e., +98.2%, whereas control C exhibits a decrease in the same phase).

This differentiation is attributed to digestion-induced changes in the phase-dependent solubility and reactivity profiles of phenolics, proteins, and reducing compounds. In addition, it may be related to the fact that DPPH is generally more sensitive to compounds with higher compatibility in organic phases (Schaich *et al.*, 2015).

On the other hand, it is widely reported in the literature that plant phenolics can be released during digestion; however, some phenolics may undergo oxidation or isomerization under near-alkaline intestinal conditions, leading to changes in their antioxidant behavior. Therefore, directional changes between phases can frequently be observed in DPPH-based assays (Wojtunik-Kulesza *et al.*, 2020).

Ferric reducing antioxidant power generally decreased during simulated gastrointestinal digestion, although the magnitude of change varied among formulations. Undigested samples exhibited FRAP values ranging from 161.80 to 1,114.53 μmol Trolox/g dm, with MI and MI-PG showing the highest initial reducing capacities. Following intestinal digestion, the FRAP values ranged between 121.68 μmol Trolox/g dm and 526.97 μmol Trolox/g dm, corresponding to reduction of approximately 25–53%, relative to the undigested state for most formulations. A notable exception was the control sample C, which exhibited a marked increase during the gastric phase prior to declining in the intestinal phase. Overall, the observed reduction in FRAP activity suggest that digestion-induced transformations may have affected compounds responsible for ferric ion reduction, resulting in lower reducing power despite the release of phenolic constituents observed in some formulations.

The general evaluation indicates that FRAP values decrease in the gastric phase for most samples (except control C), and this decrease continues in the intestinal phase, compared to the undigested state. This trend can be explained, on the one hand, by the fact that some phenolic compounds may become more susceptible to oxidation or complexation under intestinal conditions, thereby reducing their ability to reduce Fe(III). Indeed, pH and metal interactions play a critical role, particularly in polyhydroxylated phenolics. On the other hand, the presence of digestive fluids, salts, and proteins/peptides may lead to Fe binding, turbidity, and matrix-related spectral interferences in some samples, thereby suppressing FRAP readings (Everette *et al.*, 2010).

In case of blue tea-based systems, the literature has clearly demonstrated that TAC (both DPPH and FRAP) changes significantly during *in vitro* digestion. In particular, a study on butterfly pea extracts reported that the digestion process reduced both TPC and the associated antioxidant capacity (DPPH and FRAP), with this reduction being more pronounced in the intestinal phase. In the same study, it was indicated that compounds remained more stable in the gastric phase, whereas only approximately 42% of anthocyanins were retained in the intestinal phase, accompanied by a decrease in TAC (Yu *et al.*, 2024). This finding is consistent with the decrease observed in FRAP values during the intestinal phase in the present study.

However, similar to the present study, different trends are also observed in some plant-based systems. For example, in a study conducted on *Kadsura coccinea* fruits, DPPH and FRAP values increased significantly in the gastric phase (26.9–181% increase) but decreased in the intestinal phase. This indicates that antioxidant activity may increase in gastric conditions because of the release of phenolic compounds, while it may decrease in the intestinal phase because of enzymatic degradation and pH effects (Luo *et al.*, 2022).

In the present study, an increasing trend in DPPH values was observed in the intestinal phase, compared to the undigested phase. Similarly, in studies on phenolic-rich liquid food systems, such as honey, DPPH and FRAP values generally decrease after digestion; however, in some cases, the bioaccessible fraction of phenolics increases. For instance, although changes were observed in FRAP values after digestion, the total bioaccessible phenolic fraction was reported to increase within the range of 78–174%. This demonstrates that TAC depends not only on TPC but also on the chemical form and reactivity of phenolics (Seraglio *et al.*, 2017).

Overall, the literature indicates that DPPH and FRAP bioaccessibility in blue tea and similar plant-based beverages exhibit three main behaviors: (i) an increase in the gastric phase because of phenolic release, (ii) a decrease in the intestinal phase because of structural transformation and degradation, and (iii) a secondary increase in some samples depending on matrix composition and compound type. This behavior can be explained by the chemical transformations of anthocyanins and phenolic compounds during digestion and their differential contributions to antioxidant mechanisms (Yu *et al.*, 2024).

Total monomeric anthocyanin content and *in vitro* bioaccessibility

In undigested samples, TMA was found in the range of 1.39–4.45 mg/kg; the highest values were detected in MI (4.45 ± 2.28 mg/kg) and CA-PG (4.23 ± 2.33 mg/kg) samples, while the lowest value was determined in C-PG (1.39 ± 0.85 mg/kg) sample ($P < 0.05$) (Table 5). The dominant pigments of blue tea are ternatin-type polyacylated delphinidin derivatives, and the degree of acylation and environmental pH determine their color equilibrium and stability.

Although the chemical nature of ternatins (multiple acyl groups, tendency for intramolecular co-pigmentation) enhances 'blue tone' stability, they can shift between multiple equilibrium forms, such as flavylium, quinonoidal base, hemiketal, and chalcone, depending on pH.

In blue tea and similar beverages, TMA content varies widely depending on extraction method, solvent type, and processing conditions. Studies show that these compounds mainly consist of ternatin-type anthocyanins, providing strong color and antioxidant properties (Vidana Gamage *et al.*, 2021).

Kuswandari *et al.* (2022) reported total anthocyanin content of 122.79 mg/100 g in ethanol extract and 890.49 mg/100 g in freeze-dried extract demonstrated a strong effect of extraction method. In an industrial processing study, butterfly pea powder obtained by foam-mat drying reached 210 mg/100 g TMA, and encapsulation improved anthocyanin stability (Maneeratanachot *et al.*, 2024).

Similarly, anthocyanin stability varies under different pH and temperature conditions, with greater stability at pH 3.6–5.4, indicating that differences in TMA are linked to chemical transformations (Escher *et al.*, 2020).

In infusion beverages, anthocyanin content generally ranges as 10–150 mg/L, while concentrated extracts may exceed 200 mg/L. Ultrasound-assisted extraction can increase yield by 20–40% because of cell wall disruption, and anthocyanins are relatively heat-stable but sensitive to light (Vidana Gamage *et al.*, 2021).

Comparative studies in plant-based beverages show that anthocyanin content varies with formulation, and pigment stability is influenced by co-pigmentation and changes in pH (Maia *et al.*, 2025).

Overall, anthocyanins are dynamic compounds affected not only by initial concentration but also by stability and extraction conditions. Therefore, TMA results in blue tea beverages should be evaluated by considering processing method, pH, and matrix effects together.

During digestion, TMA values in both undigested and gastric phases were statistically similar, whereas intestinal digestion led to increased TMA values.

Table 5. Total monomeric anthocyanin content and *in vitro* bioaccessibility of beverage samples.

Sample	Undigested (mg/kg)	*In vitro* gastric digested (mg/kg)	*In vitro* intestinal digested (mg/kg)
C	$3.90 \pm 2.26^{d,B}$	$5.23 \pm 1.25^{c,B}$	$84.05 \pm 1.96^{d,A}$
C-PG	$1.39 \pm 0.85^{d,B}$	$5.68 \pm 1.15^{c,B}$	$77.43 \pm 10.39^{e,A}$
RO	$2.00 \pm 1.52^{d,B}$	$10.08 \pm 0.77^{a,B}$	$86.22 \pm 4.87^{c,A}$
RO-PG	$1.45 \pm 0.77^{d,B}$	$2.89 \pm 0.39^{d,B}$	$85.22 \pm 4.04^{c,d,A}$
FE	$4.01 \pm 2.89^{c,B}$	$2.23 \pm 0.19^{d,B}$	$85.50 \pm 5.47^{c,d,A}$
FE-PG	$2.50 \pm 0.87^{d,B}$	$3.78 \pm 0.51^{d,B}$	$73.75 \pm 8.45^{f,A}$
CA	$3.62 \pm 1.45^{c,B}$	$1.56 \pm 0.19^{e,B}$	$90.79 \pm 7.40^{a,A}$
CA-PG	$4.23 \pm 2.33^{b,B}$	$1.56 \pm 0.25^{e,B}$	$85.39 \pm 5.95^{c,d,A}$
MI	$4.45 \pm 2.28^{a,B}$	$2.12 \pm 0.42^{d,B}$	$87.11 \pm 1.67^{b,c,A}$
MI-PG	$1.61 \pm 1.90^{d,B}$	$2.45 \pm 0.10^{d,B}$	$87.67 \pm 2.86^{b,A}$

Notes: Values are expressed as mean ± standard deviation (SD; n = 3).
Different lowercase superscript alphabets within the same column and different uppercase superscript alphabets within the same row indicate statistically significant differences ($P < 0.05$) according to Tukey's test.
C = butterfly pea control; C-PG = butterfly pea + pepper + garlic; RO = rosemary extract; RO-PG = rosemary + pepper + garlic; FE = fenugreek extract; FE-PG = fenugreek + pepper + garlic; CA = cardamom extract; CA-PG = cardamom + pepper + garlic; MI = mint extract; MI-PG = mint + pepper + garlic.

Similarly, in a blue flower beverage + purple basil study, TMA increased in the intestinal phase (75.26–84.66 mg/kg) (Malçok *et al.*, 2025), consistent with the increase observed in the present study.

Anthocyanins were found to be more stable in the gastric phase, as also reported by Yu *et al.* (2024), where ~75.89% of anthocyanins were retained after gastric digestion. Similar stability is observed in hibiscus-based beverages (Rodríguez-Romero *et al.*, 2023).

Furthermore, acylated anthocyanins exhibit higher stability than non-acylated forms; studies on purple sweet potato showed greater stability during digestion, suggesting that ternatin-type anthocyanins in blue tea may be relatively stable as well (de Aguiar Cipriano *et al.*, 2022). Recent studies also have indicated that anthocyanin bioaccessibility depends not only on chemical structure but also on food matrix interactions with proteins and polysaccharides (Berni *et al.*, 2026).

The substantial increase observed after intestinal digestion may reflect enhanced extractability and release of anthocyanins from the beverage matrix as well as methodological effects associated with the pH differential assay following digestion. Therefore, the obtained values should be interpreted as bioaccessible anthocyanin equivalents, rather than direct evidence of anthocyanin synthesis or absolute concentration increases.

Overall, the literature indicates that anthocyanins may exhibit relative stability during the gastric phase, whereas their behavior under intestinal conditions is highly matrix-dependent and may involve degradation, transformation, or increased measurable bioaccessibility (Yu *et al.*, 2024).

Artificial neural network prediction performance and multi-response optimization

The predictive reliability of a developed ANN model was evaluated through regression and prediction analyses after the training procedure described in the 'Materials and Methods' section. As shown in Figure 5, a strong linear relationship was obtained between normalized experimental and predicted outputs, with an overall correlation coefficient of approximately R = 0.97.

The regression slope close to unity and low intercept values indicate that ANN model accurately predicted the combined responses of TMA, DPPH, FRAP, and TPC. Similar high prediction performances are reported in food systems, where ANN successfully modeled complex nonlinear relationships among processing variables and

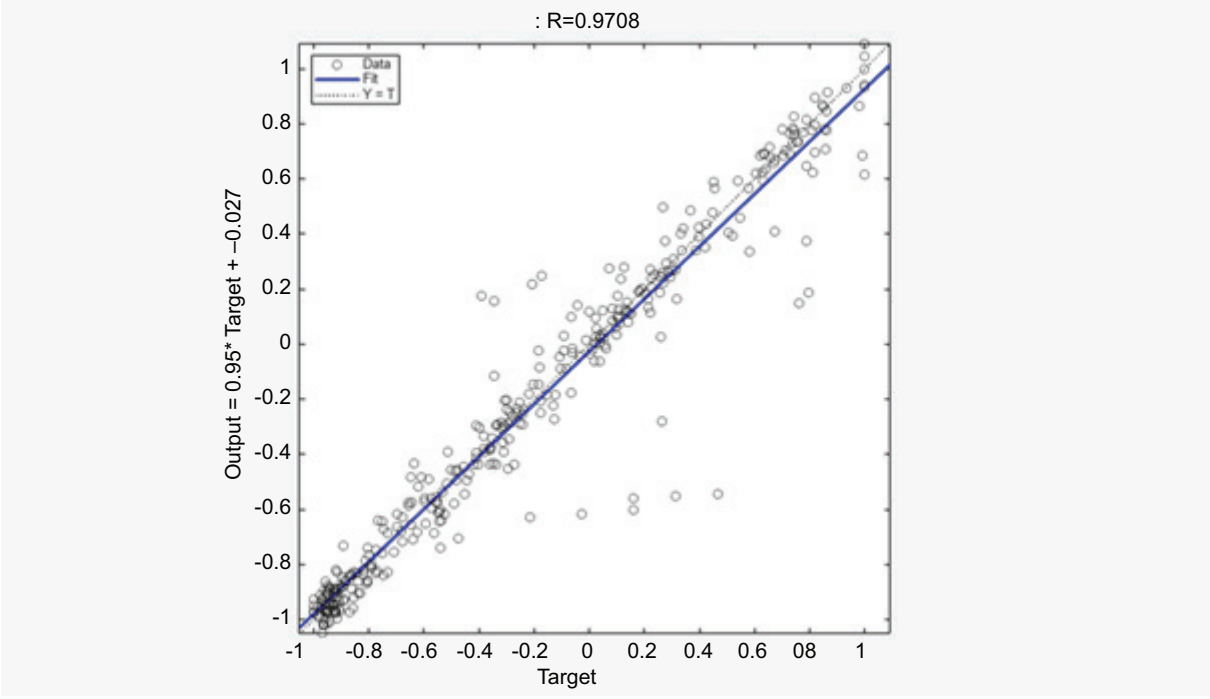

Figure 5. Regression analysis between normalized experimental and ANN-predicted values for training, validation, test, and the overall datasets.

quality attributes, particularly in drying, extraction, and formulation studies (Topal *et al.*, 2024). These findings confirm that the selected feedforward neural network (a basic type of ANN) successfully captured nonlinear interactions among formulation type, digestion stage, physicochemical characteristics, and functional quality responses.

Although a formal variable importance analysis (e.g., Garson or Olden algorithm) was not performed in the present study, the observed experimental trends suggest that the digestion phase exerted the strongest influence on TPC and antioxidant responses. Across all formulations, intestinal digestion consistently resulted in greater changes than those attributable solely to formulation differences, indicating that gastrointestinal processing was a dominant factor governing the release and transformation of bioactive compounds. This observation is consistent with the substantial increase in TPC and TAC observed following simulated digestion.

The predictive adequacy of the model was further visualized using the comparison of all normalized experimental and predicted values (Figure 6). Most data points were located close to the 1:1 reference line, confirming the high predictive ability of the model. Only a limited number of observations deviated from the diagonal line, suggesting that extreme values were more difficult to estimate precisely. Such deviations are expected in food systems because of matrix heterogeneity, digestion-induced transformations, and analytical variability. Similar deviations also are observed in previous ANN applications involving biological datasets, where sample complexity and natural variability may reduce local prediction accuracy despite strong global model performance (Inyang and Obunikut, 2022).

Following successful model validation, ANN outputs were incorporated into a multi-response optimization framework to identify the most desirable beverage formulations. It should be emphasized that the reported optimization scores do not represent direct analytical measurements; instead, they correspond to normalized composite desirability indices derived from the simultaneous evaluation of predicted TMA, DPPH, FRAP, TPC, and color quality parameters. In the present study, all responses were scaled between 0 and 1, and equal weighting was assigned to functional and color-related criteria in order to obtain a balanced optimization scenario. Multi-response desirability approaches are widely recognized as effective tools for integrating multiple quality criteria into a single decision index in food optimization studies (Baş *et al.*, 2007).

The sample-based optimization results are presented in Figure 7 and summarized in Table 6. According to the calculated composite scores, MI exhibited the highest overall desirability value (0.4955), followed very closely by FE (0.4950). Although the numerical difference between these two samples was minimal, MI provided a more balanced combination of antioxidant activity, anthocyanin retention, and phenolic content, whereas FE particularly benefited from its superior visual quality score. MI-PG ranked third (0.4741), indicating that incorporation of PG also enhanced the functional performance of this formulation. Therefore, the ranking should be interpreted as a relative prioritization, rather than evidence of a substantial practical superiority of one formulation over another. In practical applications, both formulations are considered suitable candidates, and the final selection may additionally depend on factors such as processing feasibility, ingredient availability, production cost, or specific product development objectives.

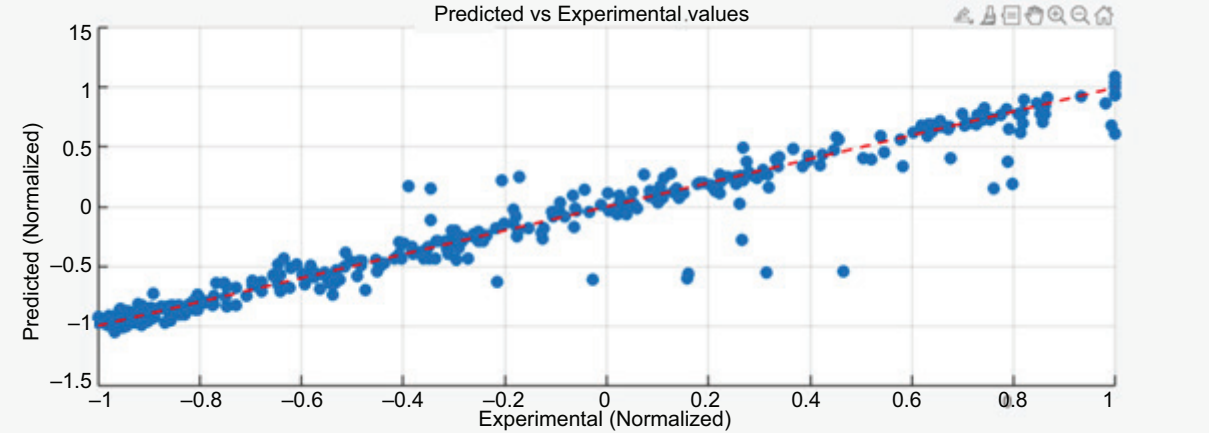

Figure 6. Comparison of normalized experimental and predicted values.

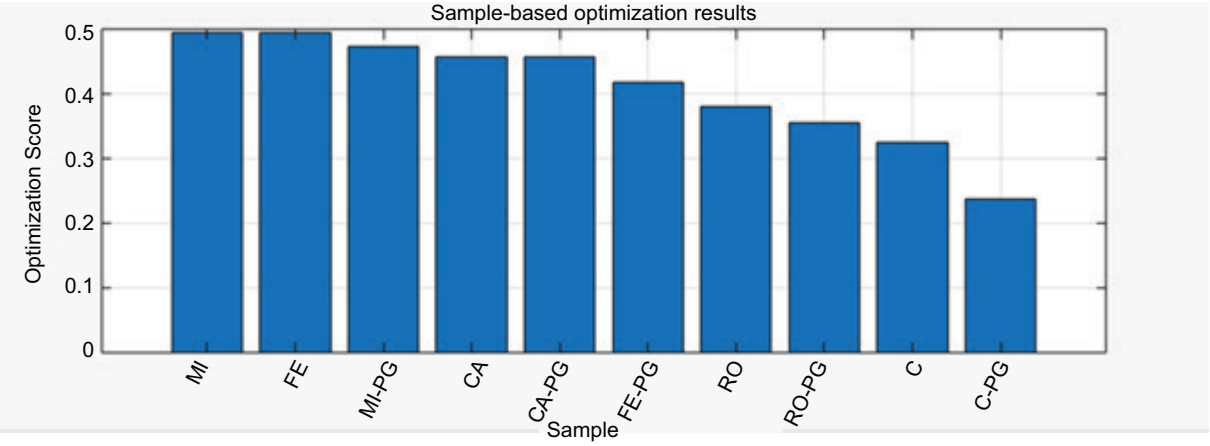

Figure 7. Composite desirability scores of beverage formulations. C = butterfly pea control; C-PG = butterfly pea + pepper + garlic; RO = rosemary extract; RO-PG = rosemary + pepper + garlic; FE = fenugreek extract; FE-PG = fenugreek + pepper + garlic; CA = cardamom extract; CA-PG = cardamom + pepper + garlic; MI = mint extract; MI-PG = mint + pepper + garlic.

Table 6. Composite desirability scores of beverage formulations obtained by ANN-based multi-response optimization.

Rank	Sample	Total score
1	MI	0.4955
2	FE	0.4950
3	MI-PG	0.4741
4	CA	0.4582
5	CA-PG	0.4570
6	FE-PG	0.4179
7	RO	0.3813
8	RO-PG	0.3565
9	C	0.3251
10	C-PG	0.2376

Notes: ANN: artificial neural network.
C = butterfly pea control; C-PG = butterfly pea + pepper + garlic;
RO = rosemary extract; RO-PG = rosemary + pepper + garlic;
FE = fenugreek extract; FE-PG = fenugreek + pepper + garlic;
CA = cardamom extract; CA-PG = cardamom + pepper + garlic;
MI = mint extract; MI-PG = mint + pepper + garlic.

In contrast, the lowest desirability values were observed for the control formulations (C = 0.3251; C-PG = 0.2376), demonstrating that relatively weak bioactive responses limited their overall optimization potential despite acceptable color characteristics.

When digestion stage was incorporated into the optimization procedure, more pronounced differences emerged among treatments. As shown in Figure 8, intestinally digested samples occupied the highest ranks. Maximum global desirability score was obtained for CA after intestinal digestion (0.6894), followed by FE-intestinal (0.6520) and CA-PG-intestinal (0.6501). These results clearly demonstrate that simulated intestinal digestion substantially improved the release and predicted availability of functional compounds in these beverages. The intestinal phase potentially promoted matrix disintegration and the liberation of bound phenolics and anthocyanins, thereby increasing measurable antioxidant responses and functional potential. Similar digestion-related increase in phenolic recovery and antioxidant bioaccessibility is widely reported for plant-based beverages and polyphenol-rich matrices (Minekus *et al.*, 2014).

The superiority of intestinal digestion conditions is further highlighted in Figure 9, where the five highest-ranked sample–stage combinations belonged to the intestinal phase. In contrast, undigested and gastric-stage samples generally showed lower desirability values, suggesting that complete release of bioactive compounds had not yet occurred prior to reaching intestinal conditions. This behavior is consistent with the progressive enzymatic degradation and pH-dependent solubilization mechanisms commonly observed during gastrointestinal digestion (Brodkorb *et al.*, 2019).

The relationship between color quality and total optimization score is presented in Figure 10. A positive but nonlinear trend was observed, indicating that superior visual appearance alone was insufficient to ensure the highest desirability score. For example, FE combined excellent color quality with strong functional responses and therefore ranked second overall. By contrast, the control sample also exhibited relatively favorable color

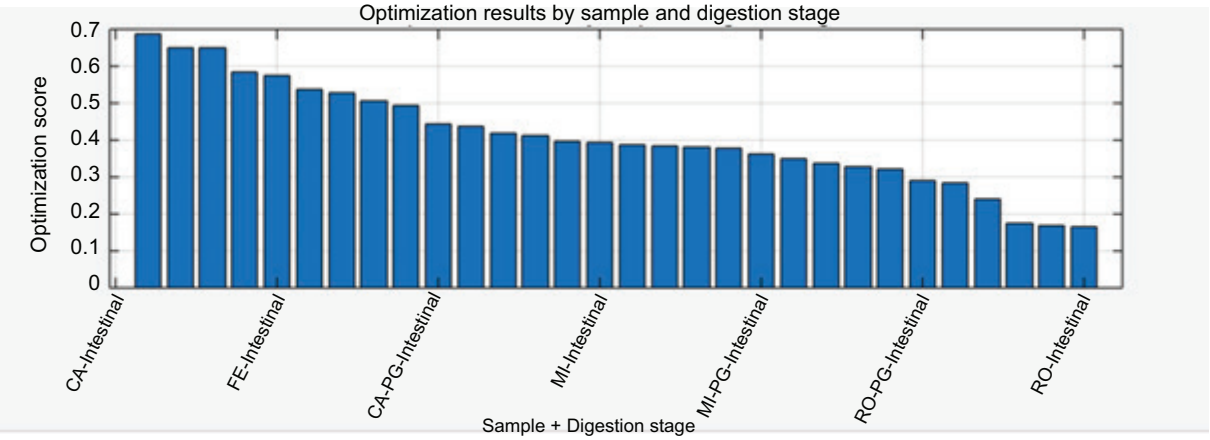

Figure 8. Composite desirability scores according to sample and digestion stage.

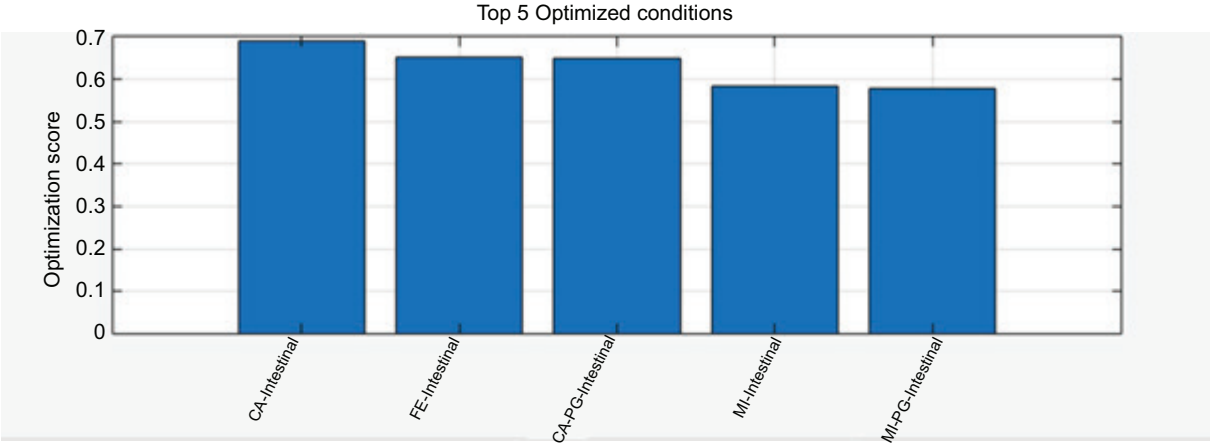

Figure 9. Top five optimized beverage formulation–digestion stage combinations.

attributes but remained in the lower ranks because of its low TPC, DPPH, and FRAP values. These findings confirm that simultaneous optimization of visual quality and functional composition provides a more realistic evaluation strategy than considering either criterion independently. Similar conclusions have been reported in functional beverage development studies, where consumer acceptability and bioactive quality must be optimized together rather than separately (Granato *et al.*, 2010).

The comparative behavior of individual predicted responses across formulations is illustrated in Figure 11. Among all responses, TPC exhibited the largest numerical variation and therefore exerted a strong influence on the final optimization score. Particularly high predicted TPC values were observed in MI-PG and CA-PG, whereas the control samples showed the lowest values. DPPH responses were highest for MI and MI-PG, while FRAP values were more evenly distributed among formulations. In contrast, TMA values varied within a narrower range than other responses, suggesting that total phenolic release and TAC contributed more strongly to the global desirability score than anthocyanin concentration alone. This observation agrees with previous reports indicating that the overall antioxidant performance in plant beverages is often governed by the synergistic contribution of multiple phenolic compounds rather than a single pigment fraction (Shahidi and Ambigaipalan, 2015).

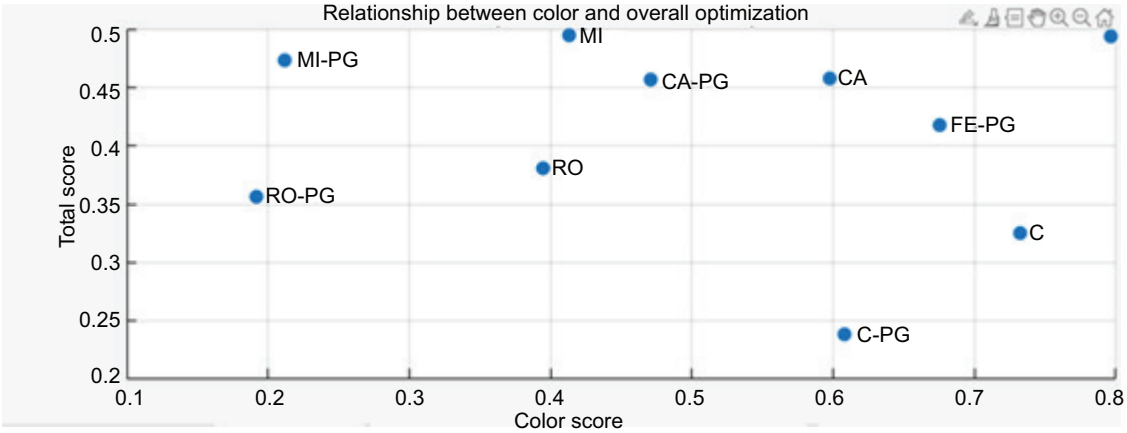

Figure 10. Relationship between color score and total optimization score. C = butterfly pea control; C-PG = butterfly pea + pepper + garlic; RO = rosemary extract; RO-PG = rosemary + pepper + garlic; FE = fenugreek extract; FE-PG = fenugreek + pepper + garlic; CA = cardamom extract; CA-PG = cardamom + pepper + garlic; MI = mint extract; MI-PG = mint + pepper + garlic.

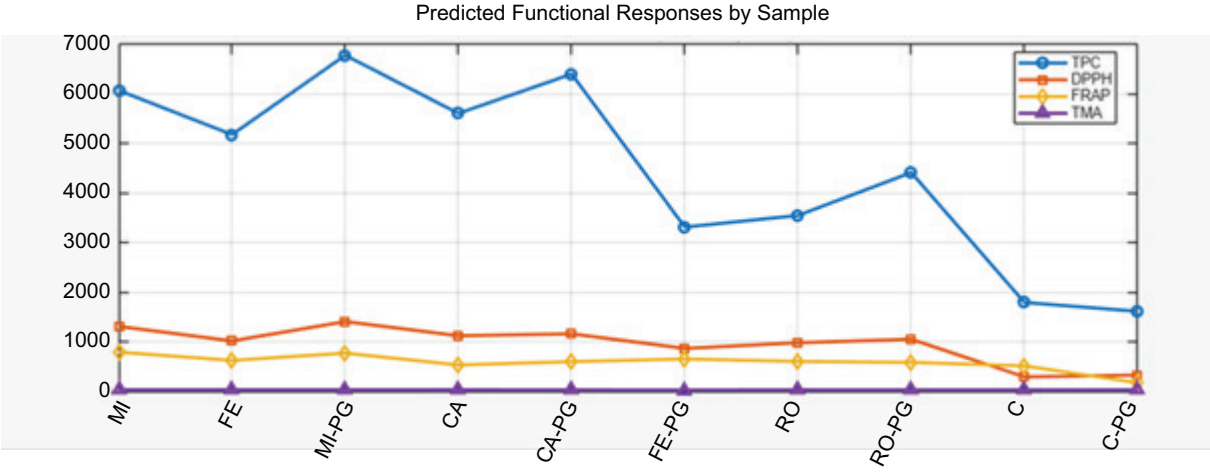

Figure 11. Predicted functional responses (TPC, DPPH, FRAP, and TMA) of beverage samples.

A holistic overview of formulation performance is provided in the heatmap (Figure 12). Higher intensity regions corresponding to TPC in MI-PG, CA-PG, MI, and CA confirm the importance of phenolic enrichment in determining optimum quality. FE showed a particularly high color score despite moderate functional response, indicating that visual quality may partially compensate for lower biochemical values in multi-response optimization. Conversely, some formulations with acceptable antioxidant capacity but weaker color properties ranked lower in the final scoring system. This demonstrates the practical value of ANN-assisted optimization, where multiple analytical and sensory-related criteria can be interpreted simultaneously.

Overall, the ANN-assisted optimization approach successfully identified the beverage formulations that best balanced functional quality, digestion-related enhancement, and desirable blue color attributes. Under the current weighting scenario, MI was selected as the optimum formulation under general conditions, whereas CA after intestinal digestion represented the best-performing sample–stage combination. These findings demonstrate that machine learning (ML)-based tools can serve as powerful decision-support systems for developing functional beverages by integrating multiple quality criteria into a single predictive framework.

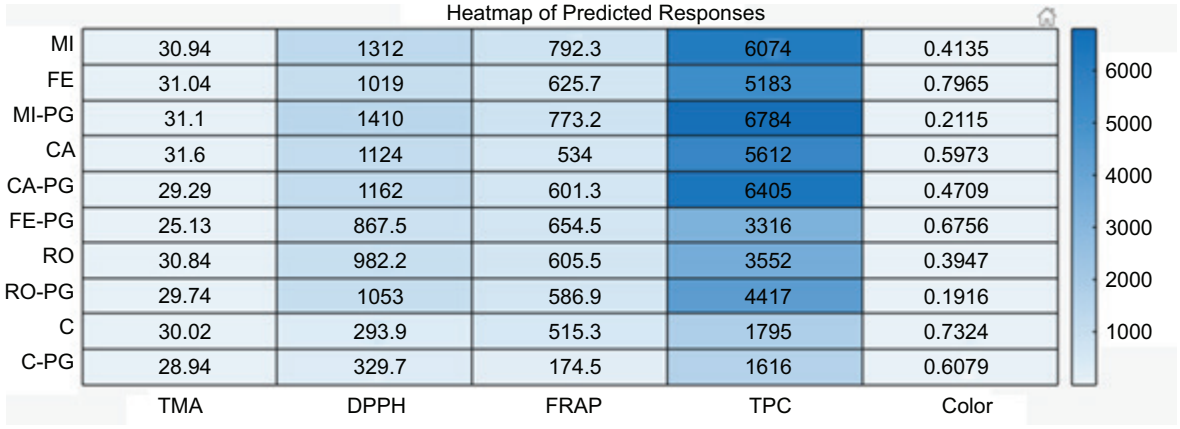

Figure 12. Heatmap visualization of predicted responses and color score. C = butterfly pea control; C-PG = butterfly pea + pepper + garlic; RO = rosemary extract; RO-PG = rosemary + pepper + garlic; FE = fenugreek extract; FE-PG = fenugreek + pepper + garlic; CA = cardamom extract; CA-PG = cardamom + pepper + garlic; MI = mint extract; MI-PG = mint + pepper + garlic.

The robustness of ANN model was supported by the consistently high predictive performance obtained for the training, validation, and test datasets, suggesting that the network successfully captured the relationships within the experimental domain. Nevertheless, the relatively limited dataset size should be acknowledged as a potential limitation. Although ANN models can be effectively applied to small experimental datasets, their predictive capability and generalizability are inherently dependent on the diversity and representativeness of training data. Therefore, the present ANN model should be considered most reliable within the range of formulation and digestion conditions investigated in this study, while additional datasets would be beneficial for further external validation and broader applicability.

Another limitation of the present study is the absence of sensory evaluation and consumer acceptability testing. Although the developed formulations were optimized based on physicochemical properties, color characteristics, phenolic content, antioxidant activity, anthocyanin content, and ANN-based desirability scores, consumer perception of taste, aroma, pungency, and the overall acceptability was not assessed. This aspect is particularly relevant for PG formulations, as these ingredients may substantially influence sensory perception and consumer preference. Therefore, the optimized formulations identified in this study should be interpreted as technologically and functionally promising candidates, while future studies should incorporate sensory profiling and consumer acceptance testing to confirm their practical market potential.

Multivariate statistical evaluation of beverage samples by PCA, HCA and correlation analysis

In order to better understand the complex relationships among physicochemical properties, functional responses, and *in vitro* digestion behavior of the developed butterfly pea beverages, multivariate statistical analyses were performed using principal component analysis (PCA), hierarchical cluster analysis (HCA), correlation analysis, and dendrogram visualization. These chemometric tools are widely applied in food systems to simplify multidimensional datasets, identify hidden relationships among variables, and classify samples according to the overall quality patterns. In beverage studies involving multiple analytical parameters, such approaches are especially useful because conventional univariate comparisons may fail to reveal interactions among variables (Cozzolino *et al.*, 2019).

Principal component analysis

The PCA results demonstrated that the first four principal components explained 88.7% of the total variance, indicating that the majority of sample variability was successfully summarized by a limited number of latent dimensions (Table 7). Specifically, PC1, PC2, PC3, and PC4 accounted for 44.3%, 21.6%, 14.1%, and 8.7% of variability, respectively. Since the first two principal components together explained 65.9% of the total variance, the PC1–PC2 score plot was considered adequate for visualizing the major patterns of sample differentiation. However, additional variability was captured by subsequent components, particularly PC3 and PC4.

Table 7. Variance ratios explained by the first four principal components.

Variables	PC1	PC2	PC3	PC4
Eigenvalue	8.4262	4.1056	2.6799	1.6488
Percentage (%)	44.3	21.6	14.1	8.7
Cumulative	44.3	65.9	80.0	88.7
Undigested TMA	0.128	0.024	0.914	–0.172
Gastric TMA	–0.471	0.276	–0.575	–0.217
Intestinal TMA	0.473	0.465	0.290	–0.511
Undigested DPPH	0.858	0.267	–0.073	0.418
Gastric DPPH	0.907	–0.172	0.327	–0.137
Intestinal DPPH	0.860	–0.250	–0.283	–0.291
Undigested FRAP	0.949	0.052	–0.028	0.249
Gastric FRAP	–0.049	0.452	0.536	0.062
Intestinal FRAP	0.947	–0.125	–0.099	0.022
Undigested TPC	0.946	0.005	–0.073	0.280
Gastric TPC	0.934	0.170	0.123	0.237
Intestinal TPC	0.872	–0.207	0.308	–0.232
L*	–0.021	–0.820	0.372	0.052
a*	–0.179	–0.827	–0.178	0.392
b*	0.495	0.733	–0.399	0.176
C*	–0.542	0.348	0.199	0.659
h°	–0.575	–0.689	0.352	0.116
pH	–0.253	0.628	0.569	0.316
TSS (°Brix)	0.610	–0.686	–0.092	0.209

Notes: TMA: total monomeric anthocyanin; FRAP: ferric reducing antioxidant power; TPC: total phenolic content; DPPH: 2,2-diphenyl-1-picrylhydrazyl; TSS: total soluble solids.

The loading matrix revealed that PC1 was primarily associated with functional quality and bioactive potential. Strong positive loadings were observed for undigested, gastric, and intestinal DPPH values, undigested and intestinal FRAP values as well as undigested, gastric, and intestinal TPC values. Therefore, samples located on the positive side of PC1 are interpreted as formulations with superior antioxidant activity and phenolic richness. Similar interpretations have been reported in functional beverage and plant extract studies, where PC1 generally reflects bioactive compound abundance and antioxidant performance.

In contrast, negative PC1 loadings were observed for C* and h°, suggesting that samples with lower chroma or shifted hue angle tended to be separated from phenolic-rich samples. This finding indicates that color behavior was not fully aligned with antioxidant performance, emphasizing the importance of simultaneously evaluating visual and biochemical quality. Accordingly, movement along the positive PC1 direction reflects increasing phenolic richness and antioxidant potential, whereas samples located on the negative side are characterized by lower functional performance and relatively greater influence of color-related attributes. Therefore, PC1 is considered the principal functional quality axis of the beverage system.

The second principal component (PC2) was mainly related to color and physicochemical attributes. Strong negative loadings were obtained for L* (–0.820), a* (–0.827), and h° (–0.689), whereas positive contributions were detected for b* (0.733), pH (0.628), and gastric/intestinal TMA. Accordingly, PC2 may be interpreted as a color-transition axis reflecting differences in brightness, blue-yellow balance, and acidity among formulations. This separation

is particularly relevant for butterfly pea beverages, where small shifts in pH and matrix composition can significantly alter anthocyanin expression and visual tone. Consequently, samples separated along PC2 primarily differ in their visual appearance and physicochemical characteristics rather than their antioxidant properties, highlighting the independent contribution of color-related attributes to the overall sample discrimination.

The PCA score plot revealed clear discrimination among beverage formulations according to both functional and color-related characteristics (Figure 13A). Samples C and C-PG were clearly separated from the spice-enriched formulations along the negative side of PC1, indicating lower antioxidant and phenolic characteristics, compared to other beverages. In contrast, MI and MI-PG were located in the positive PC1 region and were strongly associated with variables related to antioxidant activity and phenolic content. FE, FE-PG, CA, and CA-PG formed a relatively compact group in the lower-right quadrant, suggesting similar functional profiles but distinct color and physicochemical characteristics. The separation of samples along PC2 further highlights the contribution of color attributes and pH-related effects to the overall sample differentiation.

The loading plot allows for a visual assessment of the relationships between variables. Variables located close to one another indicate a positive correlation, while those positioned in opposite directions indicate an inverse correlation. Accordingly, the fact that the TPC, DPPH, and FRAP parameters are clustered in a similar region supports the notion that TAC is largely associated with phenolic compounds (Figure 13B). The close grouping of undigested, gastric, and intestinal TPC, DPPH, and FRAP variables on the positive side of PC1 indicates that these parameters were strongly associated and jointly contributed to the functional quality dimension represented by PC1. In contrast, h°, C*, and gastric TMA were positioned on the opposite side of the plot, indicating an inverse relationship with antioxidant-related variables. This separation suggests that color attributes and bioactive properties contributed independently to sample discrimination.

The third principal component (PC3) was strongly dominated by undigested TMA (0.914), indicating that the initial monomeric anthocyanin concentration behaved independently from many of other measured responses. This suggests that anthocyanin content prior to digestion was influenced more strongly by formulation composition than by the same factors governing antioxidant capacity or phenolic release. However, intestinal TMA also showed moderate contributions to PC1 and PC2, implying that digestion transformed anthocyanin behavior into a more integrated response linked with the overall bioactive profile.

Overall, the PCA results confirmed that the developed beverage samples were differentiated by two main quality dimensions: (i) functional antioxidant/phenolic capacity, and (ii) color–physicochemical behavior.

Hierarchical cluster analysis and dendrogram interpretation

The HCA dendrogram revealed three major clusters (Figure 14). The first cluster consisted of the formulations of C and C-PG, which were clearly separated from all spice-enriched beverages and therefore represented the most distinct compositional group. The second cluster included RO, RO-PG, MI, and MI-PG, indicating similarities in their overall functional and physicochemical profiles. Within this cluster, MI and MI-PG showed particularly close linkage, reflecting the similarity of their analytical characteristics. The third cluster comprised FE, FE-PG, CA, and CA-PG, suggesting that these formulations shared comparable antioxidant, phenolic, and color-related properties. The agreement between PCA and HCA confirms that formulation type was a major factor governing sample differentiation and supports the robustness of multivariate classification.

Correlation analysis

Correlation analysis revealed several strong positive relationships among functional parameters (Figure 15). Undigested TPC showed very strong positive correlations with undigested FRAP (R = 0.96), gastric TPC (R = 0.93), and gastric DPPH (R = 0.93), confirming that phenolic compounds were major contributors to antioxidant activity. Similarly, intestinal FRAP was strongly correlated with gastric DPPH (R = 0.87), gastric TPC (R = 0.85), and intestinal TPC (R = 0.79). Among color variables, h° exhibited a strong negative correlation with b* (R = –0.89), whereas L* showed a strong negative correlation with b* (R = –0.82). Furthermore, intestinal TPC displayed moderate positive correlations with b* (R = 0.58) and TSS (R = 0.60), suggesting potential interactions between soluble solids, pigment behavior, and phenolic release. Overall, the correlation structure supports PCA results by demonstrating that antioxidant-related variables formed a closely associated functional group, whereas color parameters represented a partially independent quality dimension.

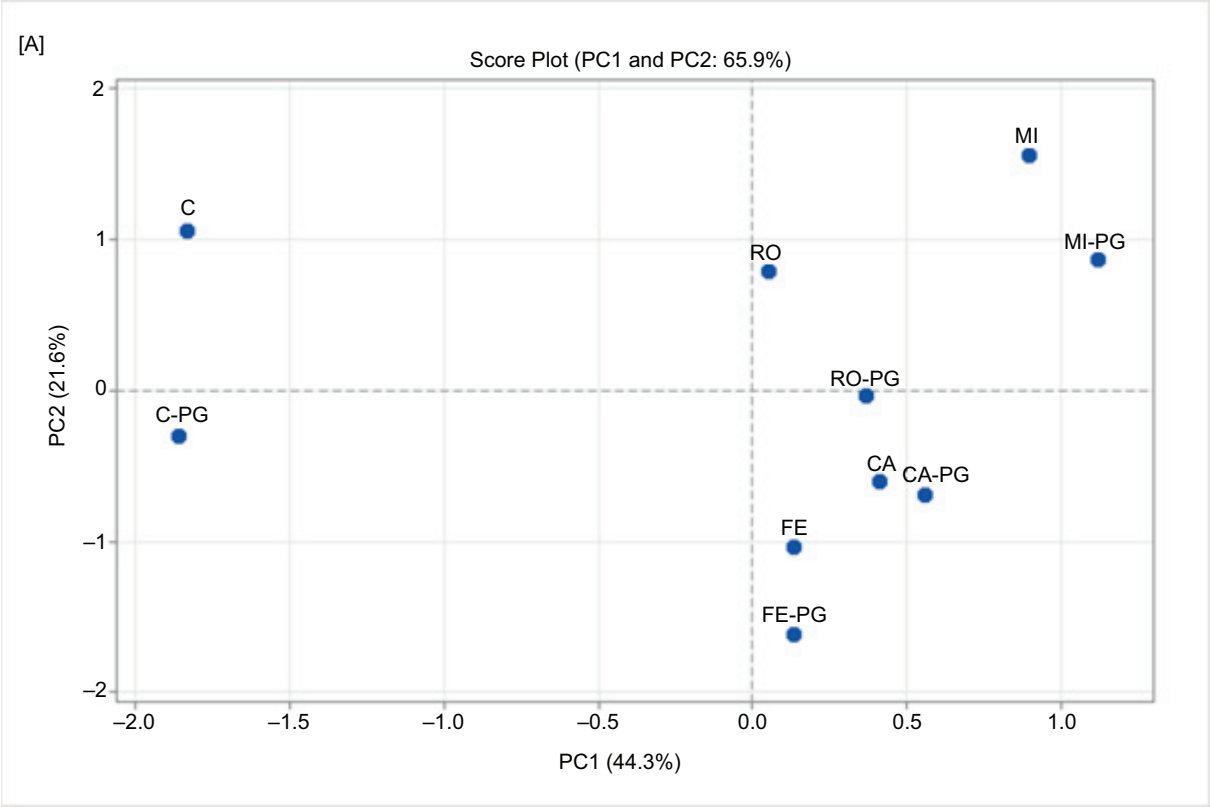

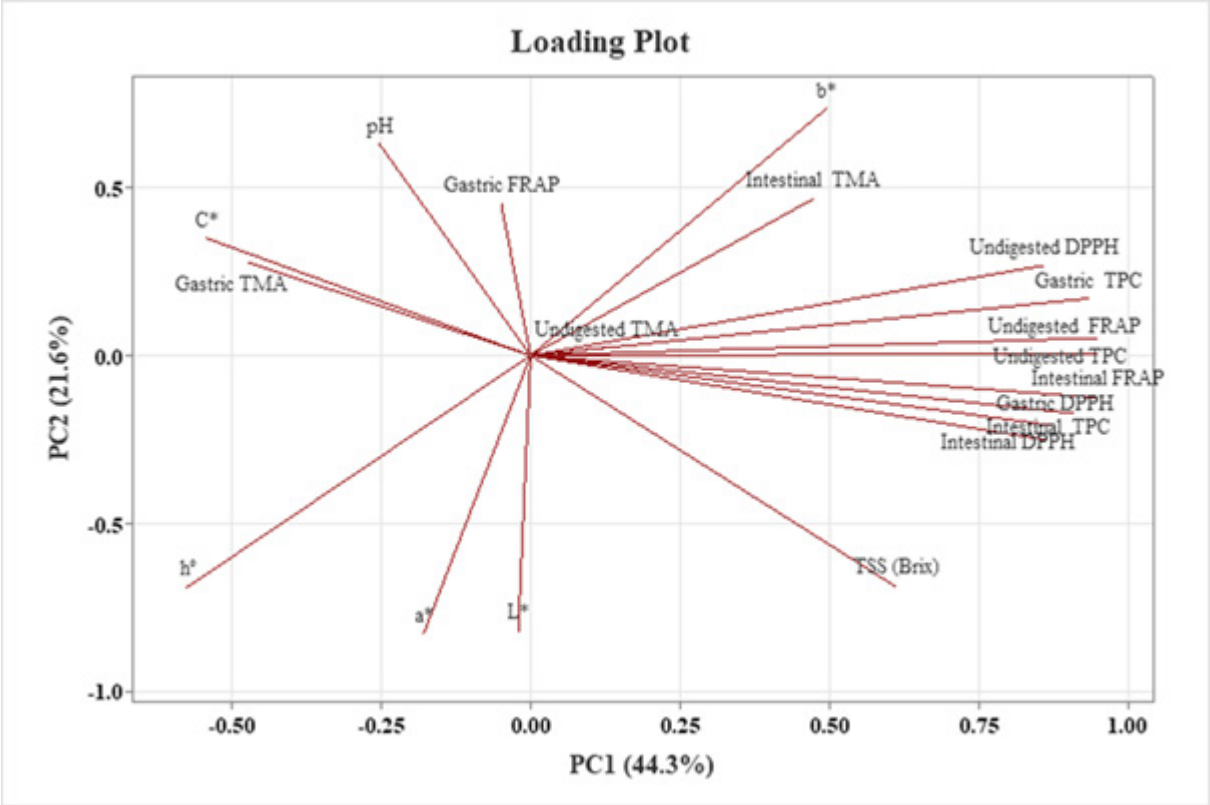

Figure 13. (A) Principal component analysis (PCA) score plot of beverage samples based on physicochemical and functional parameters; (B) PCA loading plot showing variable contributions to principal components.

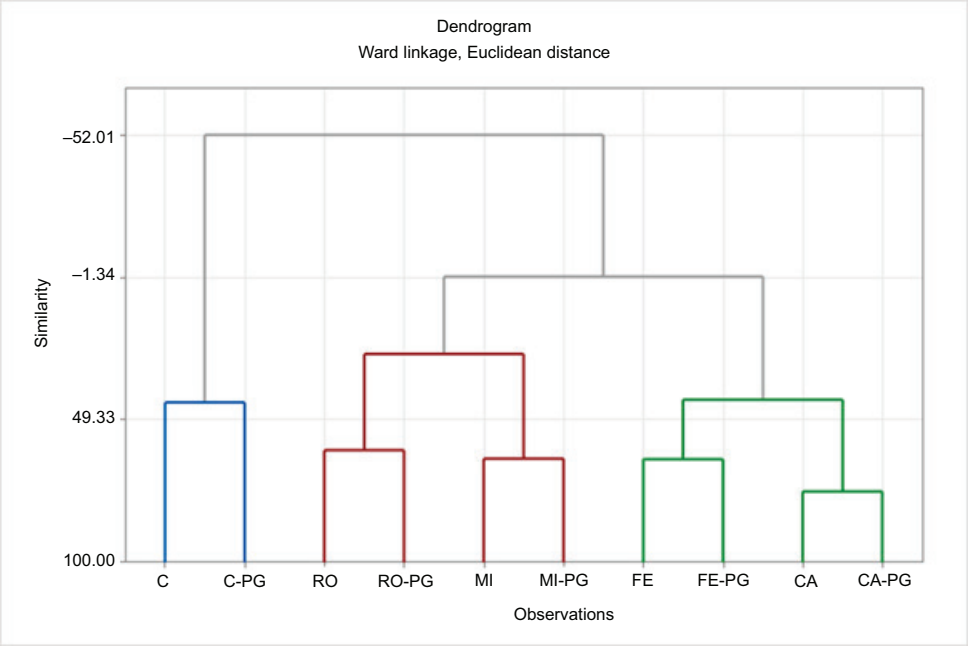

Figure 14. Hierarchical cluster analysis dendrogram of beverage samples. C = butterfly pea control; C-PG = butterfly pea + pepper + garlic; RO = rosemary extract; RO-PG = rosemary + pepper + garlic; FE = fenugreek extract; FE-PG = fenugreek + pepper + garlic; CA = cardamom extract; CA-PG = cardamom + pepper + garlic; MI = mint extract; MI-PG = mint + pepper + garlic.

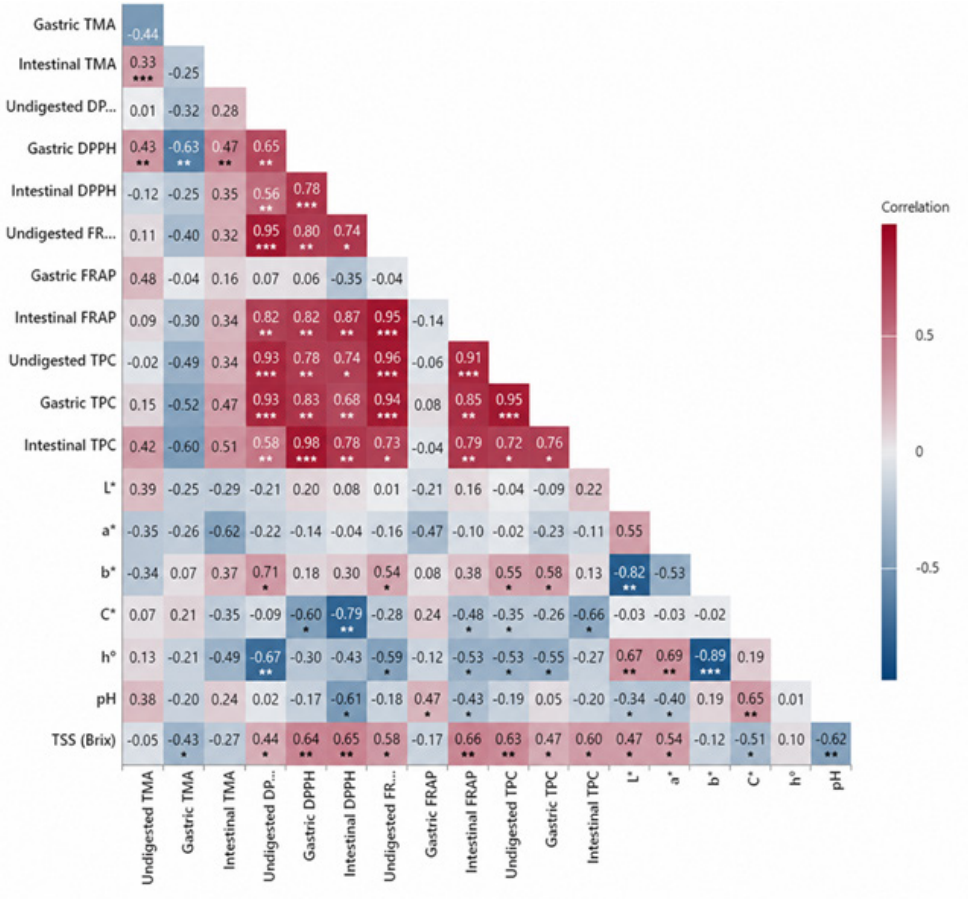

Figure 15. Pearson's correlation heatmap showing relationships among physicochemical, color, phenolic, anthocyanin, and antioxidant parameters. Significant correlations are indicated as follows: $^{*}P < 0.05$, $^{**}P < 0.01$, and $^{***}P < 0.001$.

Conclusions

This research provides a holistic evaluation of spice-enriched *C. ternatea* L. beverages, integrating advanced analytical techniques to define their quality, stability, and bioactive potential. The physicochemical analysis revealed a dynamic range of quality indicators (Brix: 0.50–1.20, pH: 5.07–6.02, and colorimetric parameters), which were significantly modulated by the spice type, underscoring the role of formulation in shaping beverage matrix. Quantitative analysis of bioactive compounds demonstrated that spice enrichment led to substantial variations in TPC (756.30–5299.33 mg GAE/100 g) and TMA (1.39–4.45 mg/kg), with a strong positive correlation between TPC and TAC, as confirmed by correlation analysis.

Multivariate statistical approaches, including PCA and HCA, provided a definitive characterization of formulations. The resulting dendrograms effectively clustered the beverages into distinct groups, highlighting how specific botanical profiles—such as mint and cardamom—exert unique influences on both pigment stability and antioxidant efficacy. Furthermore, the ANN model with an 11–10–4 topology effectively captured the complex relationships among formulation, digestion stage, and bioactive responses, achieving a high overall correlation between experimental and predicted values ($R \approx 0.97$).

The *in vitro* digestion results revealed a critical insight: gastrointestinal digestion may promote the release of phenolic compounds, resulting in a marked increase in bioaccessibility. Notably, CA-PG exhibited the highest intestinal TPC (12,813.69 mg GAE/100 g), whereas CA after intestinal digestion achieved the highest sample–stage desirability score (0.6894). In the formulation-based multi-response optimization, MI was identified as the optimal formulation for overall quality (desirability: 0.4955). These results collectively indicate that the strategic selection of spices, coupled with ANN-driven formulation optimization, provides a useful framework for the development of functional beverages with enhanced functional quality and *in vitro* bioaccessibility. This data-driven framework serves as a roadmap for the food industry to translate complex laboratory-scale findings into standardized, highly functional products.

Data Availability Statement

The datasets generated and/or analyzed during the current study are available from the author upon reasonable request.

Acknowledgments

The author expressed her deepest gratitude to late Prof. Dr. Canan Ece Tamer, whose invaluable guidance, mentorship, and inspiration profoundly shaped her academic journey.

Mandatory AI Disclosure

During the preparation of this work, the author used ChatGPT (www.chatgpt.com) in order to improve the readability and language of the manuscript. After using this tool/service, the author reviewed and edited the content as needed and takes full responsibility for the content of the published article.

Author Contributions

Senanur Durgut Malçok: conceptualization; methodology; software; validation; formal analysis; investigation; resources; data curation; writing—original draft preparation; writing—review and editing; visualization; supervision; project administration. The author read and agreed to the published version of the manuscript.

Conflict of Interest

The author declared no conflict of interest.

Funding

This research received no external funding.

References

Aksornsri, T., Chaturapornchai, N., Jitsayen, N., Rojjanapaitoontip, P. and Peanparkdee, M., 2023. Development of kombucha-like beverage using butterfly pea flower extract with the addition of tender coconut water. International Journal of Gastronomy and Food Science 34: 100825. https://doi.org/10.1016/j.ijgfs.2023.100825

Alara, O.R., Abdurahman, N.H. and Ukaegbu, C.I. 2021. Extraction of phenolic compounds: a review. Current Research in Food Science 4: 200–214. https://doi.org/10.1016/j.crfs.2021.03.010

Aljumayi, H., Sami, R., Al-Harthi, H.F., Bedaiwi, R.I., Algehainy, N.A., Almehmadi, A.M. and Qumsani, A.T. 2025. Studies of the biochemistry behavior of herbal butterfly pea blue pea flower with some antimicrobial and antioxidant potentials. Polish Journal of Environmental Studies 35(2): 2539–2547. https://doi.org/10.15244/pjoes/202196

Anggraini, T., Roza, W., Sayuti, K. and Asben, N. 2022. Potential *Clitoria ternatea* as colourant for gambir leaves tea: antioxidant activity, polyphenols, anthocyanins, catechin, and epigallocatechin gallate. International Journal on Advanced Science, Engineering and Information Technology 12(1): 379–384. https://doi.org/10.18517/ijaseit.12.1.14114

Antonio, A., Wiedemann, L. and Junior, V.V. 2018. The genus Capsicum: a phytochemical review of bioactive secondary metabolites. RSC Advances 8(45): 25767–25784. https://doi.org/10.1039/C8RA04495D

Baş, D. and Boyacı, İ.H. 2007. Modeling and optimization I: usability of response surface methodology. Journal of Food Engineering 78(3): 836–845. https://doi.org/10.1016/j.jfoodeng.2005.11.024

Berni, P., Zandoná, L.R., Berilli, P.B., Reguengo, L., Bonhin, G., Baldan, D.C. and Maróstica Jr, M.R. 2026. Bioaccessibility of anthocyanins and bioactive compounds from Brazilian berries and their food matrix interaction: an *in vitro* gastrointestinal digestion study coupled to UHPLC-ESI-TQD-MS/MS analysis. Journal of the Science of Food and Agriculture 106: 3462–3477. https://doi.org/10.1002/jsfa.70436

Borlinghaus, J., Albrecht, F., Gruhlke, M.C., Nwachukwu, I.D. and Slusarenko, A.J. 2014. Allicin: chemistry and biological properties. Molecules 19(8): 12591–12618. https://doi.org/10.3390/molecules190812591

Bouayed, J., Hoffmann, L. and Bohn, T. 2011. Total phenolics, flavonoids, anthocyanins and antioxidant activity following simulated gastro-intestinal digestion and dialysis of apple varieties: bioaccessibility and potential uptake. Food Chemistry 128(1): 14–21. https://doi.org/10.1016/j.foodchem.2011.02.052

Brodkorb, A., Egger, L., Alminger, M., Alvito, P., Assunção, R., Ballance, S., Bohn, T., Bourlieu-Lacanal, C., et al. 2019. INFOGEST static in vitro simulation of gastrointestinal food digestion. Nature Protocols 14(4): 991–1014. https://doi.org/10.1038/s41596-018-0119-1

Buvé, C., Saeys, W., Rasmussen, M.A., Neckebroeck, B., Hendrickx, M., Grauwet, T. and Van Loey, A. 2022. Application of multivariate data analysis for food quality investigations: an example-based review. Food Research International 151: 110878. https://doi.org/10.1016/j.foodres.2021.110878

Cirlini, M., Mena, P., Tassotti, M., Herrlinger, K.A., Nieman, K.M., Dall'Asta, C. and Del Rio, D. 2016. Phenolic and volatile composition of dry spearmint (*Mentha spicata* L.) extract. Molecules 21(8): 1007. https://doi.org/10.3390/molecules21081007

Cozzolino, D., Power, A. and Chapman, J. 2019. Interpreting and reporting principal component analysis in food science analysis and beyond. Food Analytical Methods 12: 2469–2473. https://doi.org/10.1007/s12161-019-01591-9

de Aguiar Cipriano, P., Kim, H., Fang, C., Venancio, V.P., Mertens-Talcott, S.U. and Talcott, S.T. 2022. *In vitro* digestion, absorption and biological activities of acylated anthocyanins from purple sweet potatoes (*Ipomoea batatas*). Food Chemistry 374: 131076. https://doi.org/10.1016/j.foodchem.2021.131076

Duque-Soto, C., Ruiz-Vargas, A., Rueda-Robles, A., Quirantes-Piné, R., Borrás-Linares, I. and Lozano-Sánchez, J. 2023. Bioactive potential of aqueous phenolic extracts of spices for their use in the food industry—a systematic review. Foods 12(16): 3031. https://doi.org/10.3390/foods12163031

Duy, N.Q., Nguyen, T.M.H., Lam, T.D., Pham, T.N. and Thanh, T.T. 2020. Extraction and determination of antioxidant activity of Vietnamese butterfly pea (*Clitoria ternatea* L.). Materials Science Forum 977: 181–186. https://doi.org/10.4028/www.scientific.net/MSF.977.181

Escher, G.B., Wen, M., Zhang, L., Rosso, N.D. and Granato, D. 2020. Phenolic composition by UHPLC-Q-TOF-MS/MS and stability of anthocyanins from *Clitoria ternatea* L. (butterfly pea) blue petals. Food Chemistry 331: 127341. https://doi.org/10.1016/j.foodchem.2020.127341

Everette, J.D., Bryant, Q.M., Green, A.M., Abbey, Y.A., Wangila, G.W. and Walker, R.B. 2010. Thorough study of reactivity of various compound classes toward the Folin–Ciocalteu reagent. Journal of Agricultural and Food Chemistry 58(14): 8139–8144. https://doi.org/10.1021/jf1005935

Fu, X., Wu, Q., Wang, J., Chen, Y., Zhu, G. and Zhu, Z. 2021. Spectral characteristic, storage stability and antioxidant properties of anthocyanin extracts from flowers of butterfly pea (*Clitoria ternatea* L.). Molecules 26(22): 7000. https://doi.org/10.3390/molecules26227000

García, M.T., Garcia-Vargas, J.M., Fernández, L.A.G., Cuevas, P. and Gracia, I. 2023. Garlic extracts: effect of pH on inhibition of *Helicobacter pylori*. Life 13(7): 1434. https://doi.org/10.3390/life13071434

Gomez, S., Pathrose, B. and Kuruvila, B. 2022. Comparative evaluation of anthocyanin pigment yield and its attributes from butterfly pea (*Clitoria ternatea* L.) flowers as prospective food colorant using different extraction methods. Future Foods 6: 100199. https://doi.org/10.1016/j.fufo.2022.100199

Granato, D., Branco, G.F., Nazzaro, F., Cruz, A.G. and Faria, J.A.F. 2010. Functional foods and nondairy probiotic food development: trends, concepts, and products. Comprehensive Reviews in Food Science and Food Safety 9(3): 292–302. https://doi.org/10.1111/j.1541-4337.2010.00110.x

Handayani, L., Aprilia, S., Arahman, N. and Bilad, M.R. 2024. Anthocyanin extraction and pH-modulated color alterations in butterfly pea flower (*Clitoria ternatea* L.). IOP Conference Series: Earth and Environmental Science 1359: 012087. https://doi.org/10.1088/1755-1315/1359/1/012087

Hariadi, H., Sunyoto, M., Nurhadi, B. and Karuniawan, A. 2018. Comparison of phytochemical characteristics pigment extract (anthocyanin) sweet purple potatoes powder (*Ipomoea batatas* L.) and Clitoria flower (*Clitoria ternatea*) as natural dye powder. Journal of Pharmacognosy and Phytochemistry 7(4): 3420–3429.

Hasanah, N.N., Mohamad Azman, E., Rozzamri, A., Zainal Abedin, N.H. and Ismail-Fitry, M.R. 2023. A systematic review of butterfly pea flower (*Clitoria ternatea* L.): extraction and application as a food freshness pH-indicator for polymer-based

intelligent packaging. Polymers 15(11): 2541. https://doi.org/10.3390/polym15112541

Inyang, U.E. and Obunikut, M.E. 2022. Artificial neural network and their applications in food materials: a review. Engineering and Technology Journal 7(4): 1–10. https://doi.org/10.47191/etj/v7i4.06

Jeyaraj, E.J., Lim, Y.Y. and Choo, W.S. 2021. Extraction methods of butterfly pea (*Clitoria ternatea*) flower and biological activities of its phytochemicals. Journal of Food Science and Technology 58(6): 2054–2067. https://doi.org/10.1007/s13197-020-04745-3

Kamiloglu, S. and Capanoglu, E. 2014. *In vitro* gastrointestinal digestion of polyphenols from different molasses (pekmez) and leather (pestil) varieties. International Journal of Food Science and Technology 49(4): 1027–1039. https://doi.org/10.1111/ijfs.12399

Kamiloglu, S., Capanoglu, E., Bilen, F.D., Gonzales, G.B., Grootaert, C., Van de Wiele, T. and Van Camp, J. 2016. Bioaccessibility of polyphenols from plant-processing byproducts of black carrot (*Daucus carota* L.). Journal of Agricultural and Food Chemistry 64(12): 2450–2458. https://doi.org/10.1021/acs.jafc.5b06094

Kenny, O., Smyth, T., Hewage, C. and Brunton, N. 2013. Antioxidant properties and quantitative UPLC-MS analysis of phenolic compounds from extracts of fenugreek (*Trigonella foenum-graecum*) seeds and bitter melon (*Momordica charantia*) fruit. Food Chemistry 141(4): 4295–4302. https://doi.org/10.1016/j.foodchem.2013.06.081

Khoo, H.E., Azlan, A., Tang, S.T. and Lim, S.M. 2017. Anthocyanidins and anthocyanins: colored pigments as food, pharmaceutical ingredients, and the potential health benefits. Food and Nutrition Research 61(1): 1361779. https://doi.org/10.1080/16546628.2017.1361779

Kim, H., Hur, S., Lim, J., Jin, K., Yang, T.-H., Keehm, I.-S., *et al.* 2023. Enhancement of the phenolic compounds and antioxidant activities of kombucha prepared using specific bacterial and yeast. Food Bioscience 56: 103431. https://doi.org/10.1016/j.fbio.2023.103431

Kumaran, A. and Karunakaran, R.J. 2006. Antioxidant and free radical scavenging activity of an aqueous extract of Coleus aromaticus. Food Chemistry 97(1): 109–114. https://doi.org/10.1016/j.foodchem.2005.03.032

Kurniawati, E., Zulfaidah, N.T., Amaliya, S.N. and Kurniawati, S.P. 2024. The effect of extraction solvents towards total flavonoid content and total phenolic content of butterfly pea (*Clitoria ternatea*) extract. Journal of Biotechnology and Natural Science 4(2): 88–94. https://doi.org/10.12928/jbns.v4i2.12158

Kuswandari, F., Sinaga, E., Nurbaiti, N. and Husni, A. 2022. Analysis of total phenols, total flavonoids and anthocyanin levels in blue pea flowers (*Clitoria ternatea* L.). Journal of Tropical Biodiversity 2(3): 152–159. https://doi.org/10.59689/BIO.V2I3.114

Lee, J., Durst, R.W. and Wrolstad, R.E. 2005. Determination of total monomeric anthocyanin pigment content of fruit juices, beverages, natural colorants, and wines by the pH differential method: collaborative study. Journal of AOAC International 88(5): 1269–1278. https://doi.org/10.1093/jaoac/88.5.1269

Li, M., Bai, Q., Zhou, J., de Souza, T.S.P. and Suleria, H.A.R. 2022. *In vitro* gastrointestinal bioaccessibility, bioactivities, and colonic fermentation of phenolic compounds in different Vigna beans. Foods 11(23): 3884. https://doi.org/10.3390/foods11233884

Luo, X., Tian, M., Cheng, Y., Ji, C., Hu, S., Liu, H., Lu, J. and Ren, J. 2022. Effects of simulated in vitro gastrointestinal digestion on antioxidant activities and potential bioaccessibility of phenolic compounds from K. coccinea fruits. Frontiers in Nutrition 9: 1024651. https://doi.org/10.3389/fnut.2022.1024651

Maia, N.M.A., Andressa, I., Cunha, J.S., Costa, N.A., Oliveira, E.B., Leite Júnior, B.R.C. and Vieira, É.N.R. 2025. *Clitoria ternatea*: perspectives on its application in foods and potential health benefits. Plants 14(21): 3322. https://doi.org/10.3390/plants14213322

Malçok, S.D., Karabacak, A.Ö., Bekar, E.R., Tunçkal, C.N. and Tamer, C.E. 2023. Influence of a hybrid drying combined with infrared and heat pump dryer on drying characteristics, colour, thermal imaging and bioaccessibility of phenolics and antioxidant capacity of mushroom slices. Journal of Agricultural Engineering 54(3): 328-342. https://doi.org/10.4081/jae.2023.1472.

Malçok, S.D., Pehlivan, E.N.H. and Tamer, C.E. 2025. Investigation of the bioactive properties and *in vitro* bioaccessibility of functional butterfly pea flower (*Clitoria ternatea* L.) beverages produced by ultrasound-assisted extraction and infusion methods. Turkish Journal of Agriculture – Food Science and Technology 13(5): 1196–1206. https://doi.org/10.24925/turjaf.v13i5.1196-1206

Maneechot, O., Hahor, W., Thongprajukaew, K., Nuntapong, N. and Bubaka, S. 2023. A natural blue colorant from butterfly pea (*Clitoria ternatea*) petals for traditional rice cooking. Journal of Food Science and Technology 60(8): 2255–2264. https://doi.org/10.1007/s13197-022-05737-6

Maneeratanachot, S., Chetpattananondh, P. and Kungsanant, S. 2024. Encapsulation of anthocyanin from butterfly pea flowers (*Clitoria ternatea* L.) extract using foam-mat drying. Food and Bioproducts Processing 145: 105–115. https://doi.org/10.1016/j.fbp.2024.03.005

Mihaylova, D., Desseva, I., Stoyanova, M., Petkova, N., Terzyiska, M. and Lante, A. 2021. Impact of *in vitro* gastrointestinal digestion on the bioaccessibility of phytochemical compounds from eight fruit juices. Molecules 26(4): 1187. https://doi.org/10.3390/molecules26041187

Minekus, M., Alminger, M., Alvito, P., Ballance, S., Bohn, T., Bourlieu, C., Carrière, F., Boutrou, R., et al. 2014. A standardised static in vitro digestion method suitable for food—An international consensus. Food & Function 5(6): 1113–1124. https://doi.org/10.1039/C3FO60702J

Muzolf-Panek, M. and Waśkiewicz, A. 2022. Relationship between phenolic compounds, antioxidant activity and color parameters of red table grape skins using linear ordering analysis.

Applied Sciences 12(12): 6146. https://doi.org/10.3390/app12126146

Nafisah, R.F., Wati, D.R., Huzainiyah, S., Agustina, E. and Purnamasari, R. 2024. Analysis of phenolic content of green tea kombucha and butterfly pea (*Clitoria ternatea* L.) flower kombucha using spectrophotometer UV-Vis. Proceedings of International Conference on Halal Food and Health Nutrition. 2(1) : 120-126. https://doi.org/10.29080/ichafohn.v2i1.2036

Nair, V., Bang, W.Y., Schreckinger, E., Andarwulan, N. and Cisneros-Zevallos, L. 2015. Protective role of ternatin anthocyanins and quercetin glycosides from butterfly pea (*Clitoria ternatea leguminosae*) blue flower petals against lipopolysaccharide (LPS)-induced inflammation in macrophage cells. Journal of Agricultural and Food Chemistry 63(28): 6355–6365. https://doi.org/10.1021/acs.jafc.5b00928

Nurhayati, R., Shoviantari, F., Munandar, T.E. and Yuwono, M. 2024. Butterfly pea (*Clitoria ternatea* L.) flower water and ethanol extract: phytochemical screening, FTIR analysis, and antioxidant activity estimation using comparison of ABTS, DPPH, and FRAP assays. Research Journal of Pharmacy and Technology 17(5): 1973–1982. https://doi.org/10.52711/0974-360X.2024.00317

Pinto, D., Ferreira, A.S., Lozano-Castellón, J., Laveriano-Santos, E.P., Lamuela-Raventós, R.M., Vallverdú-Queralt, A., Delerue-Matos, C. and Rodrigues, F. 2023. Exploring the impact of *in vitro* gastrointestinal digestion in the bioaccessibility of phenolic-rich chestnut shells: a preliminary study. Separations 10(9): 471. https://doi.org/10.3390/separations10090471

Prathumtet, J., Surasorn, C., Paopa, T. and Donthuan, J. 2018. Effect of temperature and duration of tea infusing process on total phenolic content and antioxidant activity in *Clitoria ternatea* L. flower tea. Journal of Thai Traditional & Alternative Medicine 16(3): 372–379.

Rababah, T.M., Hettiarachchy, N.S. and Horax, R. 2004. Total phenolics and antioxidant activities of fenugreek, green tea, black tea, grape seed, ginger, rosemary, gotu kola, and ginkgo extracts, vitamin E, and tert-butylhydroquinone. Journal of Agricultural and Food Chemistry 52(16): 5183–5186. https://doi.org/10.1021/jf049645z

Reis, A., Passos, C.P., Brandão, E., Teixeira, N., Alves, T., Mateus, N. and de Freitas, V. 2025. Revisiting spectrophotometric methods in the FoodOmics era: the influence of phytochemicals in the quantification of soluble sugars in plant-based beverages, drinks, and extracts. Foods 14(16): 2889. https://doi.org/10.3390/foods14162889

Rodríguez-Romero, J.J., Arce-Reynoso, A., Parra-Torres, C.G., Zamora-Gasga, V.M., Mendivil, E.J. and Sáyago-Ayerdi, S.G. 2023. *In vitro* gastrointestinal digestion affects the bioaccessibility of bioactive compounds in *Hibiscus sabdariffa* beverages. Molecules 28(4): 1824. https://doi.org/10.3390/molecules28041824

Schaich, K.M., Tian, X. and Xie, J. 2015. Reprint of "Hurdles and pitfalls in measuring antioxidant efficacy: a critical evaluation of ABTS, DPPH, and ORAC assays." Journal of Functional Foods 18: 782–796. https://doi.org/10.1016/j.jff.2015.05.024

Seraglio, S.K.T., Valese, A.C., Daguer, H., Bergamo, G., Azevedo, M.S., Nehring, P., *et al.* 2017. Effect of *in vitro* gastrointestinal digestion on the bioaccessibility of phenolic compounds, minerals, and antioxidant capacity of *Mimosa scabrella Benthamhoneydew* honeys. Food Research International 99: 670–678. https://doi.org/10.1016/j.foodres.2017.06.044

Shahidi, F. and Ambigaipalan, P. 2015. Novel functional food ingredients from marine sources. Current Opinion in Food Science 2: 123–129. https://doi.org/10.1016/j.cofs.2015.01.003

Shi, C., Zhao, Z., Jia, Z., Hou, M., Yang, X., Ying, X. and Ji, Z. 2024. Artificial neural network-based shelf life prediction approach in the food storage process: a review. Critical Reviews in Food Science and Nutrition 64(32): 12009–12024. https://doi.org/10.1080/10408398.2023.2245899

Sitompul, J.N. and Martati, E. 2025. The physicochemical properties of butterfly pea flower (*Clitoria ternatea* L.) extracts: influence of various extraction conditions. Journal of Experimental Life Science 15(3): 97–105. https://doi.org/10.21776/ub.jels.2025.015.03.01

Tagliazucchi, D., Verzelloni, E., Bertolini, D. and Conte, A. 2010. *In vitro* bio-accessibility and antioxidant activity of grape polyphenols. Food Chemistry 120(2): 599–606. https://doi.org/10.1016/j.foodchem.2009.10.030

Topal, M.E., Şahin, B. and Vela, S. 2024. Artificial neural network modeling techniques for drying kinetics of *Citrus medica* fruit during the freeze-drying process. Processes 12(7): 1362. https://doi.org/10.3390/pr12071362

Vidana Gamage, G.C., Lim, Y.Y. and Choo, W.S. 2021. Anthocyanins from *Clitoria ternatea* flower: biosynthesis, extraction, stability, antioxidant activity, and applications. Frontiers in Plant Science 12: 792303. https://doi.org/10.3389/fpls.2021.792303

Wahyanto, K.N. and Agustini, R. 2024. Total flavonoid content and in vitro anti-inflammatory potentials of kombucha with enrichment of butterfly pea (*Clitoria ternatea*) flower extract. Jurnal Pijar Mipa 19(2): 254–259. https://doi.org/10.29303/jpm.v19i2.6320

Widyawati, P.S., Suseno, T.I.P., Ivana, F., Natania, E. and Wangtueai, S. 2024. Effect of butterfly pea (*Clitoria ternatea*) flower extract on qualities, sensory properties, and antioxidant activity of wet noodles with various composite flour proportions. Beverage Plant Research 4: e022. https://doi.org/10.48130/bpr-0024-0011

Windarsih, Y., Budiarsa, I.M., Trianto, M., Akram, A. and Ashari, A. 2025. Analysis of nutritional composition and antioxidant activity of yogurt enriched with butterfly pea (*Clitoria ternatea* L.) extract. Biology, Medicine and Natural Product Chemistry 14(2): 831–841. https://doi.org/10.14421/biomedich.2025.142.831-841

Wojtunik-Kulesza, K., Oniszczuk, A., Oniszczuk, T., Combrzyński, M., Nowakowska, D. and Matwijczuk, A. 2020. Influence of *in vitro* digestion on composition, bioaccessibility and antioxidant activity of food polyphenols—a non-systematic review. Nutrients 12(5): 1401. https://doi.org/10.3390/nu12051401

Yu, F., Yu, Q., Yin, N., Sun, G., Peng, Y., Zeng, Y. *et al.* 2024. *In vitro* and *in vivo* evaluating bioaccessibility, bioavailability, and antioxidant activities of butterfly pea flower containing bioactive constituents. Foods 13(10): 1485. https://doi.org/10.3390/foods13101485

Zhou, H., Tan, Y. and McClements, D.J. 2023. Applications of the INFOGEST *in vitro* digestion model to foods: a review. Annual Review of Food Science and Technology 14(1): 135–156. https://doi.org/10.1146/annurev-food-060721-022040

Zor, M., Şengül, M., Karakütük, İ.A. and Aksoy, S. 2023. Investigation of various infusion conditions on physical, chemical and antioxidant properties of *Clitoria ternatea* L. tea. Journal of the Institute of Science and Technology 13(3): 1738–1754. https://doi.org/10.21597/jist.1267541